AFFDL-TR-68-170

PLASMA DIAGNOSTIC METHODS FOR IONIZED GAS FLOWS

Final Report

C. FORBES DEWEY, JR.
University of Colorado, Boulder, Colorado

TECHNICAL REPORT AFFDL-TR-68-170

March 1969

AIR FORCE FLIGHT DYNAMICS LABORATORY
AIR FORCE SYSTEMS COMMAND
WRIGHT-PATTERSON AIR FORCE BASE, OHIO

NOTICE

When Government drawings, specifications, or other data are used for any purpose other than in connection with a definitely related Government procurement operation, the United States Government thereby incurs no responsibility nor any obligation whatsoever; and the fact that the Government may have formulated, furnished, or in any way supplied the said drawings, specifications, or other data, is not to be regarded by implication or otherwise as in any manner licensing the holder or any other person or corporation, or conveying any rights or permission to manufacture, use, or sell any patented invention that may in any way be related thereto.

This document has been approved for public release and sale; its distribution is unlimited.

Copies of this report should not be returned unless return is required by security considerations, contractual obligations, or notice on a specific document.

AFFDL-TR-68-170

PLASMA DIAGNOSTIC METHODS FOR IONIZED GAS FLOWS

Final Report

C. F. FORBES DEWEY, JR.
University of Colorado, Boulder, Colorado

FORWARD

This report is a summary of work completed under Contract No. F33615-67-C-1850, Project No. 26692, "Plasma Diagnostic Methods for Ionized Gas Flows" in the Aerospace Engineering Sciences Department, University of Colorado, Boulder, Colorado. The Principal Investigator was C. Forbes Dewey, Jr., and the Contract Monitors were Dr. Paul Polishuk and Mr. Rudy C. Beavin.

This technical report has been reviewed and is approved.

H. W. BASHAM
Chief, Control Elements Branch
Flight Control Division
Air Force Flight Dynamics
Laboratory

ABSTRACT

An investigation has been conducted to elucidate several different methods of diagnostics for ionized gas flows. Particular emphasis was placed on techniques of possible interest to the 50 Megawatt Facility at Wright Field.

An analysis was completed which describes the behavior of Langmuir probes in strong magnetic fields. The detailed behavior of the results indicates that the theory is capable of describing, with reasonable quantitative accuracy, the collection properties of Langmuir probes as a function of applied potential and magnetic field strength for all magnetic fields $B > 0$.

Thomson scattering measurements of electron density do not appear feasible for the 50 Megawatt Facility for two reasons. First, the large fluctuations in plasma density (from less than 10^5 to approximately 10^{12} cm^{-3}) measured in the facility during the time period of this contract makes Thomson scattering an extremely difficult measurement to perform (the lower limit of electron density for Thomson scattering is roughly 10^{12} cm^{-3}). And second, the estimated contamination levels (on the order of 10^{-2} to 10^{-1} wt. percent of contaminants) would introduce spurious signals which will be of the same order as the electron scattering.

An analysis was made of several types of atomic and molecular flourescence radiation experiments of potential diagnostics use in the 50 Megawatt Facility. It is concluded that local specie concentration measurements of NO and O_2 can be accomplished using laser flourescence excitation, and that gas velocity measurements can be made using laser excitation of the N_2 Lyman - Birge - Hopfield system or the NO (β) system and monitoring the trajectory of the excited volume of gas.

Additional work completed during the contract and described herein is as follows:

(1) A novel method of "pumping" energy conversion devices with lasers to acheive enhanced electrical output.

(2) A general survey of laser sources for line spectroscopy.

(3) A new method of joining porous refractory metals.

(4) Laser welding.

TABLE OF CONTENTS

I. ELECTROSTATIC PROBES IN MAGNETIC FIELDS

This investigation was undertaken to clarify the role of magnetic fields in influencing the behavior of electrostatic probes in magnetic fields. Previous theories were inadequate and not grounded on a consistent approach to the kinetic equations of plasmas; rather, they were ad hoc models which exhibit anomalous (and often even qualitatively incorrect) results when compared to experiment.

The results of this investigation are detailed in AFFDL-TR-67-190, January 1968, entitled "Theory of a Probe in a Strong Magnetic Field" by J. R. Sanmartin. The "exact" theory is treated in the limiting case of $B \to \infty$ and represents a clear interpretation of the reduction in collected current arising from the imposed magnetic field. Of particular importance is that even moderate fields of a few hundred Gauss can substantially alter the collected current and hence the plasma density inferred from the probe current-voltage curve. Although the theory is formally valid only for the limiting case of a strong field, the results appears to be applicable to weaker fields as well. This occurs because the form of the results agrees in the limit $B \to 0$ with the classical limit for a collisionless fully-ionized plasma without a magnetic field. In particular, the theory should be applicable to assessing the effects of existing magnetic fields on Langmuir probe characteristics in the low-density sections of the 50 Megawatt Facility.

II. THOMSON SCATTERING

One of the objectives of this contract was to examine the feasibility of Thomson scattering as a method of measuring electron density and

static temperature in the 50 megawatt facility. In addition to relatively straightforward applicational calculations, it was intended to perform suitable feasibility experiments on a fully-ionized laboratory plasma of the Q-machine type. Experimental difficulties surrounding the physical construction of the Q-machine prevented the experiments from being performed, although the calculations were completed.

The applicational calculations may be summarized as follows. Under the most ideal laboratory conditions (including extensive refinement of the optical paths introduced into the vicinity of the measurement point), it should be possible to measure electron thermal temperatures via doppler width and density via total scattered signal using a pulsed ruby laser and Thomson scattering, at electron densities exceeding $2\text{-}5 \times 10^{12}$ cm^{-3}. However, measurements conducted by the personnel of the 50 megawatt facility during the time period of this contract suggest that the lower limit given above is in fact the upper limit of the fluctuating electron density in the 50 megawatt facility. This precludes effective use under the non-ideal operating conditions encountered in this large operation with "hostile" gas environments for the delicate optical fixturing.

Another important point is the contamination level of the flow. Solid particles (copper, molten metal, carbon, dust, etc.) act as diffuse scatterers with effective cross-sections many orders of magnitude larger than the electrons. An estimate of the maximum contamination of micron-size solid particles which would yield scattering signals of the same magnitude as the electron Thomson scattering signal (assuming 10^{-5} ionization fraction) is on the order of 10^{-7} wt%. This is several orders of magnitude

less than the published estimates of contamination for the 50 megawatt facility.

In summary, the Thomson scattering measurement technique is an excellent laboratory tool for "clean" conditions, but appears not to be feasible for the 50 megawatt facility at electron densities below about 10^{15} cm^{-3}.

III. SPECIE DENSITY MEASUREMENTS

During this contract an extensive survey of laser sources and optical techniques amenable to spectroscopic measurements was conducted. This review, plus some pertinent applications, are detailed in Attachment A.

The results indicate that laser sources are suitable for flourescent scattering experiments involving air species, and the scattering signals can be interpreted to yield information on local species number densities and velocities of flowing, low-density gases.

The general features of the scattering technique and laser sources are presented in the attachment. In this section, we present the results of typical calculations directly applicable to the 50 megawatt facility.

In performing the calcualtions, the following "typical" free-stream conditions have been assumed:

$$M_\infty = 7.5$$

$$V_\infty = 3600 \text{ m/s}$$

$$T_\infty = 500 \ ^oK$$

$$\rho_\infty = 5 \times 10^{-6} \text{ gm/cm}^3 \text{ (air)}$$

$$N_e = 10^{10} \text{ cm}^{-3}$$

Then the total particle density is roughly 1.1×10^{17} cm^{-3} for all species. The flow may be highly nonequilibrium, particularly with regard to the equilibration of vibrational and translational degrees of freedom. From current data on vibrational relaxation, it is estimated that for the conditions cited above the vibrational degrees of freedom will "freeze out" at approximately 2000 ^{o}K during the nozzle expansion, whereas the translational temperature will continue to drop to around 500 ^{o}K in the test section. The magnitude of the rotational temperature will be discussed shortly.

This freezing is very important because flourescent scattering from molecules in the visible and near ultraviolet region accesssible to laser sources depends strongly on the populations of the various vibrational levels of the ground-state molecules. As a general rule, the Franck-Condon overlaps (which are roughly proportional to the absorption cross-sections) for transitions between molecular ground states and excited states are larger for higher vibrational quantum numbers, and the Boltzmann factor $\exp - [E(v)/kT_{vib}]$ gives the population of the upper levels relative to the vibrational ground state. Here E(v) is the energy of the v^{th} vibrational level relative to the ground vibrational state. For O_2, for example, at 500 ^{o}K, the Boltzmann factor corresponding to $v = 5$ is about 10^{-10} whereas at 200 ^{o}K it is 10^{-2}.

Some of the prominent air species and spectroscopic bands investigated are as follows:

O_2 (Schumann-Runge) [abbreviated O_2(SR)]

NO (γ)

NO (β)

N_2 (Lyman - Birge - Hopfield) [abbreviated N_2(LBH)]

In the calculations summarized below, we have used the spectroscopic data of S. A. Golden [J.Q.S.R.T., 7, 225 (1967)] and R. A. Allen (AVCO Research Report 236, April, 1966) plus some unpublished calculations from the reentry physics group at TRW Systems (L. Hromas, M. Jenuehomme, et al.).

Two band systems which appear particularly promising are the O_2(SR) and NO(γ). The presence of NO at the representative free-stream conditions cited previously can only occur from a freezing of specie concentrations during the expansion process, and consequently nonequilibrium mass fractions. From a comparison with similar calculations for reentry flow fields, one might expect free-stream concentrations on the order of 1% NO and roughly 10% O_2 (rather than the 20% at equilibrium). From the point of view of interpreting the results of heat-transfer and aerodynamic studies in a frozen, partially-dissociated free stream, it is important to know the concentration of O_2 and, to a lesser extent NO. The importance of O_2 is obvious. The role of NO is two-fold; first, accurate prediction of the NO concentration is a sensitive test of the ability of the nozzle analysis to predict "freezing"; and second the heat of formation of NO is on the order of 0.6 eV/molecule, or about the same as the kinetic energy of the particles at $M_\infty = 7$ and $T_\infty = 500\ ^\circ K$. If the NO concentration were abnormally large, some systematic errors in the interpretation of heat transfer measurements could be expected. Furthermore, relaxation

phenomena about slender-body flow fields could be substantially altered.

At a vibration-rotation temperature of 2000 ^{o}K the O_2(SR) absorption is nearly continuous over the entire infrared spectrum, having a peak of α^* 0.3 cm^{-1} $atm.^{-1}$ at 1880 $\overset{o}{A}$, a short-wavelength cutoff at about 1750 $\overset{o}{A}$, and dropping monotonically from the peak as one progresses to longer wavelengths. However, it is not clear that such will be the case for expanding nozzle flows. It is surmized that $T_{vib} >> T_{rot} \quad T_{transl.}$, and in this case the O_2(SR) absorption bands will show dramatic structure with strong peaks at the band heads corresponding to each vibrational transition ($\nu^1 \rightarrow \nu^{11}$), with little of the continuous structure corresponding to excited rotational levels.

NO(γ) absorption for $T_{vib} = T_{rot} = 2000$ ^{o}K exhibits strong peaks at each band head, and this will be accentuated if $T_{vib} >> T_{rot}$. The maximum absorption coefficient at $T_{vib} = 2000$ ^{o}K is in the neighborhood of 2300 $\overset{o}{A}$, i.e. O_2 and NO absorption (and flourescent emission) can occur at the same wavelengths. <u>The relative magnitudes of the two absorptions depend critically on the exact wavelength of the laser excitation and the rotational and vibrational temperatures.</u> If $T_{rot} << T_{vib} \quad 2000$ ^{o}K, then Q-switched lasers with powers on the order of 0.1 to 1 megawatt and tunable over small frequency ranges in the 2100 $\overset{o}{A}$ - 2300 $\overset{o}{A}$ range should produce very good measurements of NO and O_2 densitites because, without the intra-band rotational structure, the band-head absorption peaks of O_2 and NO are very sharp and there should be negligible overlap. One should, in fact,

be able to obtain the vibration temperature by individual measurements at different lower vibrational levels.*

If $T_{rot} \sim T_{vib} \sim T_{transl.} \sim 500\ ^{o}k$, then the O_2(SR) flourescence measurement becomes impossible because the absorption coefficients for the $\nu'' = 0$ vibrational level are too small; then O_2(SR) absorption measurement requires either $\nu'' \geq 5$ or <u>very</u> short wavelength excitation (the (0,0) transition for O_2(SR) is at 2076 $\mathring{A}$), and no tunable sources of high power have been uncovered below about 2300 $\mathring{A}$. The only possibility would be to use Q-switched liquid dye lasers and attempt to generate third harmonics.

Density measurements with O_2(SR) and NO(γ) resonance flourescence are feasible because the natural lifetimes are 0.8×10^{-8} sec and 1.2×10^{-7} sec. respectively, i.e. short compared to the time required for the flow to move across the laser-excited interaction volume.

IV. <u>SPECIE VELOCITY MEASUREMENTS</u>

The basic philosophy behind laser excitation to effect velocity measurements in flowing gases is given in pp. 47 and 48 of <u>Attachment A</u>.

---

*Perhaps the most promising laser source for NO(γ) is a hybrid beam produced by mixing ruby second-harmonic at 3471 $\mathring{A}$ with N_2 2nd-positive radiation at 3371 $\mathring{A}$ in an ADP crystal to produce an output at 2266 $\mathring{A}$. This is virtually coincident with the NO(γ) (0, 0) band head at 2265.6 $\mathring{A}$. (See Allen, loc eit.). Some authors list this band head at 2275 $\mathring{A}$, and the discrepancy appears unresolved.

The comments given below present the conclusions of calculations based on the typical operating condition of the 50 megawatt facility as listed at the beginning of Section III.

It is clear that the 0_2(SR) and NO(γ) bands have lifetimes which are too short for tracking purposes, 10^{-8} and 10^{-7} sec. respectively. A review of the lifetimes of all air specie band systems has revealed that selective excitation (as contrasted with "massive" excitation - - - see Attachment A) can be most profitably be used with the N_2 Lyman - Birge - Hopfield, N_2(LBH), system and the NO(β) system.

The first consideration has to do with focussing and tracking the excited volume of gas. Consider a sharply-delineated blob of gas of diameter d_o to be excited by the laser. This can either be a point of focus (rather speherical volume) or a thin cylinder of gas excited by a parallel beam. The "blob" spreading angle α

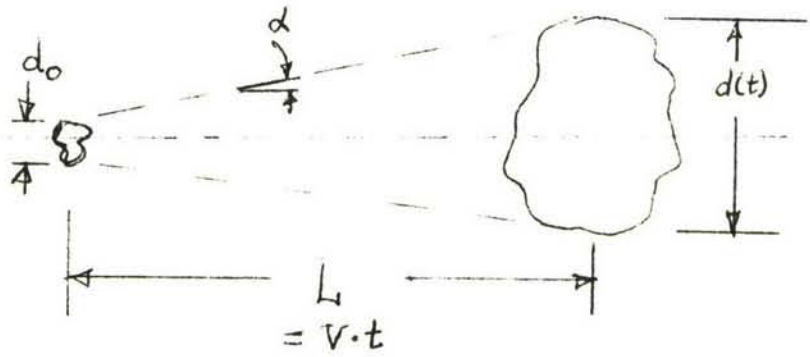

has a maximum value which is determined by the ratio of the thermal velocity to the mean velocity V which is to be measured. We have, for $M_\infty >> 1$,

$$d(t) \approx d_o + 2L\left(\frac{1}{M_\infty}\right)$$

$$\approx d_o + \frac{2Vt}{M_\infty}$$

A measurement of L and t determines V, whereas measurement of L, t, d_o, and d(t) yield V and M_∞, or V and T_∞ if γ is known. If the spreading is purely by diffusion of the dilute excited state concentration, then the blob growth is quite small and governed by the local diffusion coefficient.

With "massive" excitation, an enormous energy is deposited in the flow and a translating spherical blast wave of rather uncertain composition and dimension is produced. The spreading angle α is very large and the accuracy of the measurement of V is poor. L. Rittenhouse at AEDC has claimed a very nigh accuracy for this technique in a private conversation, but from the above argument it appears that this accuracy is open to serious question. On the other hand, the amount of energy deposition per unit volume using selective line excitation is very small, and only a small perturbation of the flow would be expected.

Computations for the excitation of N_2(LBH) were based on Allen's spectroscopic estimates:

Oscillator Strength $f = 0.37 \times 10^{-5}$

Natural Lifetime $\tau = 1.7 \times 10^{-4}$ sec.

(0, 0) Band Head $\tilde{\nu}_\infty = 68948.3$ cm^{-1}

We assume a parallel laser beam produced by second-harmonic generation from a nitrogen second-position laser, with a resulting wavelength of 1686 Å.

Using 2.5 MW for 4ns for the primary beam (J. D. Shipman, Jr., Appl. Phys. Lett., 10, 3 (1967)) and 10% harmonic conversion, the input power is equal to 2×10^{14} photons/pulse.

For the standard conditions listed previously, a vibration-rotation temperature of 2000 ^{o}K, and estimating the absorption coefficient to be 3.5×10^{-5} cm^{-1} $(atm\ N_2)^{-1}$ from extrapolating the calculations of Allen for the (1, 5) band of the N_2(LBH) system at 1686 $\mathring{A}$, there are 2×10^{7} excited states produced per cm of laser path.

The smallest practical spot size for large focal distances (on the order of 1 to 2 meters) is about 0.13 cm. For $(L/d_o)_{max} = 20$, an assumed free-stream velocity of 3.6×10^{5} cm/sec., and assuming spreading at the Macangle, the time of flight to L = 2.6 cm is 7μs and $d(7\mu s) \sim 0.9$ cm. The total number of photons radiated from this volume at L during the time it traverses its own diameter is 4×10^{5}. Assuming that the detector optics intercept a solid angle of 2.4×10^{-2} steradians of the isotropic flourescent radiation, there will be approximately 10^{3} photons intercepted by the detector. An oscilliscope trace of the detector output would appear as follows:

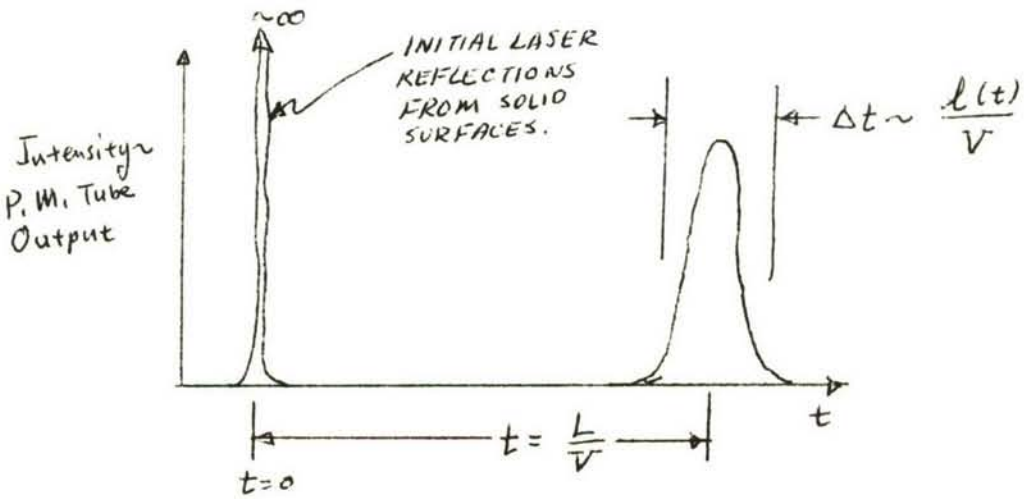

In order to discriminate against background radiation, a relatively narrow-band filter should precede the detector. Because of the short wavelength and low rate of photon emission, the optical system must be of rather high quality. However, one compensation is that τ is so long that the total radiation from the excited blob decays very slowly and L may be easily changed without requiring compensation for the attenuation of the total emission intensity. Also, there are no other significant band system of air which radiate below 1750 $\mathring{A}$, and the signal will be very pure, uncontaminated by background radiation.

In the case of pure diffusion of the blob, the growth of an excited cylinder of gas will be parabolic with distance, and as a rough estimate (based on a Lewis number of unity) will not grow to more than twice the original diameter in a distance equal to 20 d_o. Coupling this result with a natural lifetime of $\tau = 1.7 \times 10^{-4}$ sec., the N_2(LBH) radiation can be tracked for at least 20 cm in the downstream direction. This long path length allows either discrete data on the time-of-flight for given distances, or an image-converter streak camera picture of the blob trajectory. A sequence of lenses and light pipes could be used to define different points in the downstream direction.

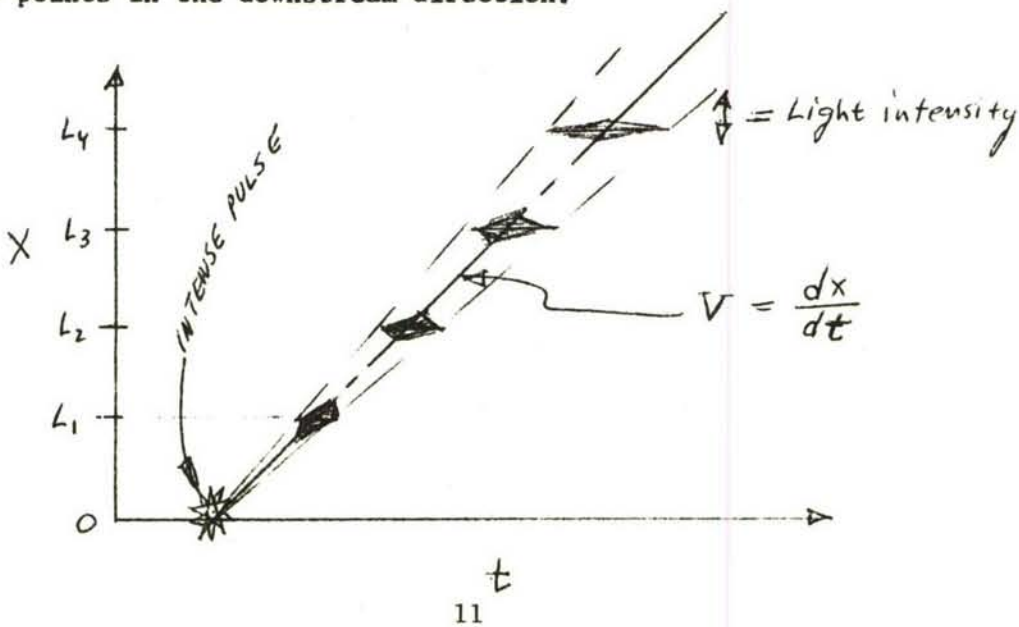

The preceding calculations for N_2(LBH) illustrate techniques which are useful for large natural lifetimes, i.e. $\tau \sim 10^{-4}$ sec. Intensities are relatively low because of the slow decay rate, but the excited blob can be tracked for long distances. There are no prominent band systems from air with $\tau \sim 10^{-5}$ sec. However, NO(β) has a natural lifetime $\tau = 0.67 \times 10^{-6}$ seconds, and in spite of the low NO concentration which will exist in the free-stream of the 50 megawatt facility, the absorption and emission rates are larger than those obtained with N_2(LBH)

Calculations for NO(β) have been completed assuming 1% NO frozen into the flow during expansion, and using

$$f = 0.01 \text{ (oscillator strength)}$$

$$\tau = 0.67 \times 10^{-6} \text{ sec. (lifetime)}$$

$$\tilde{\nu}_{\infty} = 45440.0 \text{ cm}^{-1} \text{ [(0,0) band head frequency]}$$

Several laser sources were investigated and the absorption computed using the calculated spectroscopic distributions of Allen for $T_{vib} = T_{rot} = 2000$ °K. The most favorable absorption is achieved using the Ruby 3rd harmonic at 2314 Å which excites NO(β) near the (2,2) band head. Using a 2MW pulse over 10 ns. as the ruby 3rd harmonic input (see Attachment A), and the standard conditions detailed earlier, approximately 0.6×10^{11} excited states will be produced per cm of laser beam travel. The initial isotropic flourescence would be 0.9×10^{17} sec^{-1} per cm of beam length, a very intense source compared to the N_2(LBH) flourescence. However, the rapid decay of intensity with distance precludes following the blob over large distances; the decay rate has dropped to 0.4×10^{9} sec^{-1} per cm of length

at L = 5 cm. Furthermore, following the rapidly-changing intensity in time requires a highly nonlinear detection scheme because the intensity drops by roughly one order of magnitude for each 1/2 cm of travel in the streamwise direction. The most expedient method of handling this problem is with a sequence of light pipes along the flow direction having attenuation filters whose density is an exponentially decreasing function of distance from the point of excitation. In that manner the relative detector response to the flourescent signals will be of the same order of magnitude along the length of observation.

The technique of selective laser excitation for velocity measurements is intrinsically much more attractive than the massive excitation technique whereby a laser produces a spark by gas breakdown in the flow field. In addition to the higher reproducibility and potential accuracy, the selective excitation is feasible in high-temperature air from about 10^{-3} atmospheres up to 1 atmosphere and above. Massive excitation requires higher and higher laser excitation power as the pressure decreases, and the approximate scaling law below 1 atmosphere is

$$P_{Laser} \sim \rho_{\infty}^{-1}$$

V LASER PUMPING OF ENERGY CONVERTERS

During this contract an investigation was initiated into the possibility of enhancing plasma density by laser excitation. The basic ideas behind these techniques and a specific application to cesium-filled thermionic energy converters are given in Attachment B.

The basic scheme is to produce a highly non-equilibrium gas by pumping laser energy into atomic excitation. The excited atoms, being

within a few kT_e of the ionization limit, are subsequently ionized by electron collisons. The laser excitation of atoms from a lower excitation level to a highly-excited level is in fact the direct inverse of the physical process leading to radiative recombination by radiative cascading, and therefore laser excitation can be used to balance both radiative and collisional recombination in a plasma. The recombination rate can be written

$$\frac{dn_e}{dt} = - \alpha(n_e, T_e) n_e^2$$

where $\alpha(n_e, T_e) = \alpha(T_e)$ for radiative recombination and $\alpha(n_e, T_e) = n_e \alpha^*(T_e)$ for purely collisonal recombination. Regardless of the details of the recombination process, an enhanced excitation rate to states near the continuum will yield, in steady-state, an increased plasma density so that the recombination and excitation rates, including both collisonal, radiative, and external laser contributions, are once again in balance.

The calculations given in Attachment B suggest that significant increases in output power can be achieved in thermionic diodes by using laser excitation. Whether the additional power exceeds that required to operate the laser is still open to question. However, the potential gains in efficiency are very attractive and are being pursued by the writer at the present time under other sponsorship.

Other applications of the laser plasma production scheme are also being investigated under another aegis. A paper entitled "Plasma Ionization Enhancement by Laser Radiation" by P. E. Oettinger and

C. F. Dewey, Jr. will be presented at the AIAA Aerospace Science Meeting in New York in January, 1969.

VI. SURVEY OF LASERS AND LASER TECHNIQUES

The pursuit of the above-named topic resulted in the completed survey included as Attachment A. This paper has been submitted for publication.

VII. LASER WELDING

Laser welding techniques were investigated at a low level of effort throughout the duration of the contract. Although oft-times our efforts had the character of a "re-invention of the wheel," we learned a great deal about laser welding fabrication possibilities and developed several new techniques which, to the best of my knowledge, have not been explored elsewhere.

Our primary contribution was to develop a simple and reliable method of welding refractory metals into vacuum-tight configurations of a relatively large scale. Our greatest success was achieved in tantalum-tantalum welds, although other metal combinations (W-W, Ta-SS, Mo-SS, Mo-Mo, Cu-Cu, etc.) were successfully treated.

Continuous seam welds were produced by laying down a series of overlapping spot welds, as illustrated in the photograph appearing as Fig. 1. This picture illustrates a larger degree of overlap than is necessary to produce a vacuum-tight and mechanically sound joint; the minimum successful overlap was found to be about 50-60% for conditions where the diameter of the individual weld nugget was about equal to the minimum thickness of the two pieces being joined. For thick sections and small spot diameters, the degree of overlap must be increased.

Our experimental plasma assembly required vacuum-tight circular welds of up to 10" in circumference. Both pieces involved in the joint were tantalum, and normally one was a thin shell of 0.005-0.008" thickness and the other a massive (0.100"-0.250" thick) support structure. Our previous experience with electron-beam and inert atmosphere arc welding was singularly unsuccessful. The special jigs and fixtures required to align the pieces were expensive and time-consuming to make. The large heat inputs caused warping and misalignment of the delicately-fitted joints during the welding process. Residual stresses arising from non-uniform temperatures of the part during welding led to unsatisfactory mechanical properties and poor life under cyclical loads. Severe grain growth occurred in the welded parts because of the very high temperatures encountered in these two processes. And finally, the electron-beam process was extremely expensive because of the large capital investment in the equipment (~$100,000.)

The laser used in this welding system was a Raytheon LE-8 with a LPS-21 power supply and several additional energy storage capacitors and pulse-forming inductors added to increase the pulse length. The total system investment was approximately $16,000, including a home-made optical system for focussing the ruby output and viewing the work, a small vacuum bell jar for performing welds in a controlled atmosphere, and a rotating workpiece table mounted inside the bell jar and powered with a 3 volt motor from a small electric toy automobile.

The welding operation consisted of three phases: (1) Aligning the optical system, (2) "tacking" the weld with widely-spaced spots along

its length, and (3) laying down an overlapping series of spot welds to produce the seam weld itself.

Alignment was carried out on a test configuration to determine the optimum pulse length, spot size (i.e. degree of beam defocus), pulse total energy, and overlap. A sharp focus and/or a short pulse length produced holes in the joint, with molten metal being literally blown out of the crater by vaporized material. Too long a pulse length increased the total energy required and increased the width of the heat-affected zone surrounding the weld. Although this sounds like a very "arty" process, an empirical optimization was usually rapidly achieved and nearly identical results could be obtained for $\pm$ 20% changes in energy, time, spot size, and degree of overlap. During an actual weld, however, it is important to obtain reproducibility from shot to shot on the order of $\pm$ 5% or better to insure a weld of uniform properties.

Tacking was used to reduce progressive buildup of errors in the alignment of the joint. It was found on circumferential welds (at least with a thin member on the outside of the joint) that there was a progressive and additive "stretching" of the material which produced a severe mismatch between the pieces near the end of the welding operation. The effect was similar to spinning or creeping, but its exact origin is unknown.

Once the weld area was aligned under the laser beam and the parts tacked in place, the actual welding process was routine. The DC motor of the rotation table was connected across a capacitor which was charged to a predetermined voltage. Each pulse of the laser produced a command pulse to a relay which discharged the small capacitor across

the motor and advanced the rotary table through the required angle, thus readying the work piece for the next pulse. A positive ratchet-and-pawl arrangement would have been equally satisfactory. The weld was checked visually through the viewing optics every 20-40 shots to verify proper alignment of the weld bead with respect to the joint.

All of our successful welds with refractory metals were accomplished in an inert gas atmosphere. Before welding, the vacuum chamber was evacuated to 50 μ and backfilled to atmospheric pressure with laboratory-grade argon or helium, and this cycle was repeated several times to insure that O_2 and N_2 concentrations were below 20 ppm. The bell jar was then filled to about 50 mm Hg above atmospheric pressure for the duration of the welding, and a small relief value allowed a purge flow of about 5 cfm to continuously sweep through the chamber. Welds produced in the atmosphere with refractory metals were brittle, weak, and had very poor reproducibility. O_2 and N_2 embrittlement are well-known in refractory metal technology.

The simplicity of set-up and the case of operation of the laser welder suggests a bright future for this method of fabrication for one-of-a-kind assemblies as well as production items. To illustrate the simplicity, we had a Freshman join the group as a laboratory assistant, and within one week he was producing successful laser welds on a variety of assemblies. Repairing and rewelding across previously-melted areas can also be accomplished, but the experience level required is considerably higher.

Joint configurations appear to be of less importance than the mechanical tolerances of the joint. As in electron-beam welding or any other process where large energy deposition rates are involved, a poor mechanical fit with poor heat conduction paths will lead to asymmetric melting and "blow-through" rather than fusion between two melted pieces. For laser welding, the energy deposition rates are extremely high and mechanical tolerances are at a premium. Some of the successful Ta-Ta joint configurations used in this program are illustrated below.

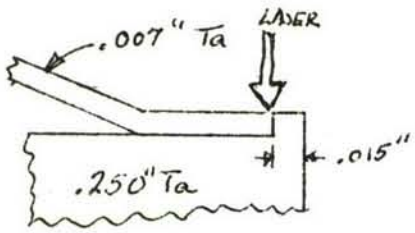

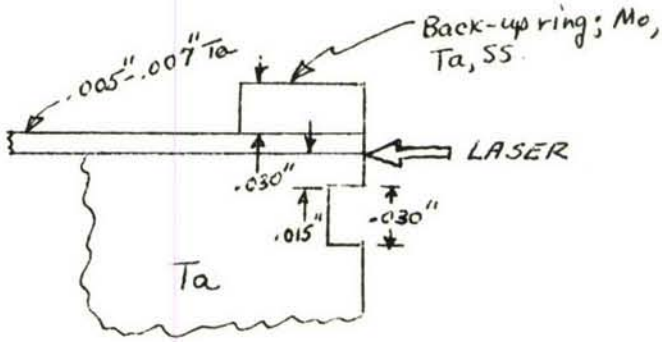

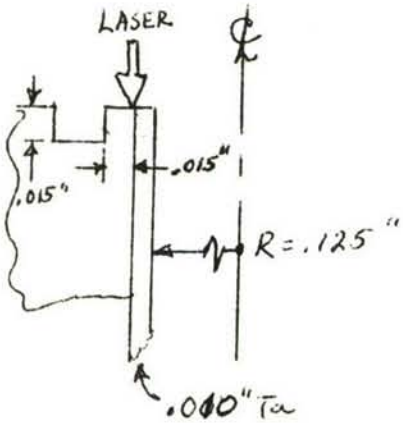

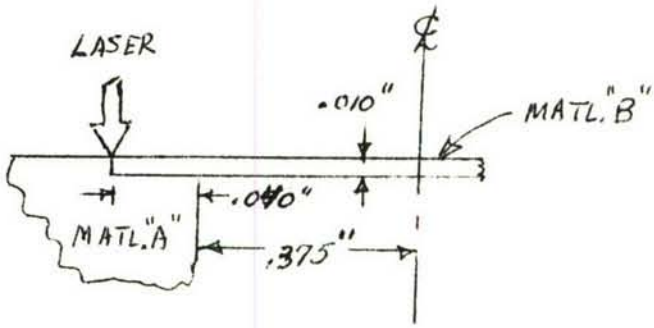

NOTE: ALL CIRCULAR INSERTS FRICTION FIT.

MATL. "A"	MATL. "B"
Ta	Ta
Mo	Mo
S.S.	Ta
S.S.	S.S.
S.S.	Mo
W	W

VIII POROUS MATERIAL FABRICATION

The extremely difficult technological job of fabricating the porous emitter for our Q-machine was finally accomplished near the end of our contract period, but not in time to allow full operation of the cesium plasma.

Two major fabrication problems existed. The first was to weld the several separate pieces into a vacuum-tight configuration. This was finally achieved by using the laser welding techniques described in the preceding section. The second problem was to develop a method of sealing the porous emitter to the tantalum support shell. The final successful method of accomplishing this is described in Attachment C. Several potentially important applications of this technique are suggested in the attachment.

IX. ACKNOWLEDGEMENTS

It is a pleasure to acknowledge the important contributions which were made to the work reported here by the following individuals:

J. R. Sanmartin, Research Assistant

D. L. Hanse, Instrument Maker

C. R. Younger, Research Assistant

G. R. Smith, Research Assistant

P. E. Oettinger, Post-Doctoral Fellow, Joint Institute for Laboratory Astrophysics.

J. P. Gravier, Research Assistant

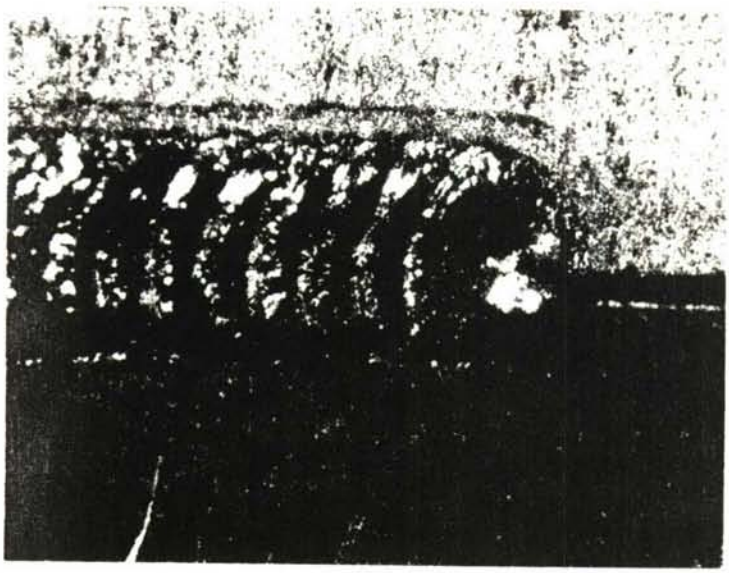

Fig. 1. Photograph of $\approx 0.1''$ wide laser weld between tungsten and tantalum.

ATTACHMENT A

APPLICATIONS OF LASERS TO LINE SPECTROSCOPY

by

C. Forbes Dewey, Jr.*

University of Colorado, Boulder, Colorado

ABSTRACT

Recent advances in semiconductor lasers and frequency-changing methods have significantly broadened the wavelength spectrum in which laser energy can be generated. A review of available techniques in the visible and near-infrared is presented. At the present time, it appears possible to produce intense coherent radiation at all wavelengths from 1700 Å to 16μ. Applications to line spectroscopy and plasma diagnostics are described.

*Present Address: Department of Mechanical Engineering, Massachusetts Institute of Technology, Cambridge, Massachusetts.

I. INTRODUCTION

Application of lasers to atomic line spectroscopy has been severely restricted in the past because of the very low probability that any available laser wavelength will exactly match the wavelength of the particular spectroscopic line of interest. The widths of spectroscopic and coventional laser lines are often less than a few tenths of an Angstrom, and very little wavelength tuning can be accomplished in conventional CW gas lasers or solid-state laser materials such as rubies or Nd^{+}-doped glasses.

This paper reviews several new developments which promise to remove these difficulties in the visible and near-infrared wavelength spectrum. The primary limitations appear to be the short pulse times available (10 to 300) nano-seconds) and the small total energy of the output (2×10^{-7} to 10^{-1} Joules per Angstrom bandwidth) for methods which allow continuous tuning of the output wavelength. Nonlinear techniques for multiplying the number of discrete laser frequencies available are also discussed.

In any particular spectroscopic application, laser light sources must compete with improved flash lamps which have been developed in recent years. Although broad-band applications presently favor the use of flash lamps, continued progress in the laser methods reviewed in this paper may soon reverse this plurality. For excitation of discrete lines a few Angstroms or less in width, laser intensitites far exceed those available from flash lamps.

The main emphasis of this paper is directed to frequency-changing methods for discrete laser wavelengths, including temperature variation of the lasing

medium and nonlinear optical techniques. The final Section is devoted to calculations showing application to particular diagnostic problems in plasmas and high-temperature flowing gases. Although the characteristics of semiconductor lasers are discussed extensively, more conventional laser mediums such as ruby, Nd-doped glasses, and He-Ne and other gases are not described. There are excellent references available reviewing the operating characteristics of this latter category (see e.g. B. A. Lengyel[1]).

II. CHARACTERISTICS OF SEMICONDUCTOR LASERS

In the last 4 years, a whole host of semiconductor materials have been induced to efficiently emit coherent laser radiation at room temperature and below. Instead of "pumping" via an external light source, these lasers are excited most expediently either (a) with large reverse current through standard p - n junctions, or (b) by electron-beam injection perpendicular to homogeneous semiconductor crystals. Figs. 1 and 2 present typical arrangements for the two schemes. Ivey[2] presents a rather dated survey of semiconductor compounds exhibiting laser action, and additional citations are given by Morehead.[3] Because of the active development presently going on in the semi-conductor laser field (particularly in the investigation of the effects of crystal purity) it is to be expected that subsequent results will outmode the present discussion.

GaAs, a favorable example of semiconductor lasers suitable for spectroscopy, has several interesting properties. First, it exhibits a high efficiency of conversion from electrical to light energy, up to 80% at 77 ^{o}K.[3] Second, the radiation bandwidth is relatively narrow, on the order of 1 $\overset{o}{A}$ at 77 ^{o}K and 5 $\overset{o}{A}$ at 300 ^{o}K[4]. Third, the output wavelength is tunable by

(1) temperature variation, (2) changes in impurity concentration, (3) changes in composition, and (4) the application of pressure or a magnetic field. And fourth, the diodes are extremely compact, occupying less than 1 cm^3 for an average output power of 10 mW.

Wavelength tuning is particularly important to this application because a precise match must be achieved between the shifted and broadened atomic excitation of interest and the laser light source. Pure GaAs can be temperature-tuned from about 8000 Å (4.2 °K) to 9050 Å (300 °K) although the conversion efficiency drops to 2-5% at room temperature. Superimposed on this variation is a shift in output wavelength by $\pm$ 85 Å with different impurity concentrations. Ternary compounds offer an additional method of wavelength variation; the combination $GaAs_xP_{1-x}$ ($0.5 \leq x \leq 1$) at 77 °K would cover the spectral range 6300 Å to 8450 Å. Fine tuning via magnetic fields is possible but has not been extensively investigated.

Significant laser power outputs from semiconductors were reported as early as 1963. Garfinkel and Engler[5] produced 1.5 watts CW in a GaAs diode with a conversion efficiency of 30%, and Lax[6] developed 100 watts in pulsed operation. Commercial units are now available in this range, with laboratory prototypes producing considerably higher outputs (up to 800 watts peak power).

Fig. 3 is a diagrammatic summary of the semiconductors which have been investigated for use as lasers. Compounds in which lasing action has been observed or is highly probable cover the spectrum from 3245 Å to 16μ. Fig. 4 gives the observations of Hurwitz[7] for the compound CdS_xSe_{1-x}, which covers the wavelength interval 4900 Å - 6900 Å. The data at 4.2 °K

and 77 ^{o}K suggest the range of wavelength tuning achievable with temperature changes; for this compound the difference is about 15 Å, the wavelength increasing with temperature. Temperatures intermediate to these points should be achievable with proper heat sink arrangements, the use of liquid helium and small heating coils, or by thermoelectric cooling.

The main limitation to pulse length is the rate at which the sample temperature rises during the excitation pulse. Hurwitz[8] and Nicol[9] have observed electron-beam excited sample temperatures to rise as much as 80 ^{o}K during a 0.2 micro-second pulse, causing shifts of about 20 Å in the emitted wavelength over the duration of the pulse. Gonda, Junker, and Lamorte[10] find the line shift in GaAs to be about 0.3 Å (amp^{2} - μs)$^{-1}$ during reverse-current excitation. This sweeping may be advantageous in guaranteeing coincidence between a particular spectral line and the laser line, but the effective pulse length may be reduced to a fraction of a nanosecond if the spectral line is very sharp. Wavelength shifts from heating may be minimized by employing sharp, short excitation waveforms which reach thresholds rapidly. The duty cycle is limited by the average power dissipation within the laser material.

Spectroscopic applications involving very sharp atomic lines, i.e. ones with a total half-width on the order of a few tenths of an Angstrom, or less, are made more difficult by the fact that the outputs of semiconductor lasers exhibit a very complicated mode structure. Fig. 5[11] is a resolved output line of Zn S, one of 10 such simultaneous output lines to be observed. The output peaks would sweep successively across a narrow spectroscopic line as the lasing medium temperature rose with continued excitation.

Absorption or scattering signals would therefore exhibit an extremely high modulation rate.

At the present time, GaAs is the only semiconductor laser to be marketed commercially, and the development of other compounds as operational spectroscopic light sources will require considerably more demand than presently exists. In many applications, however, the coherence and directivity of laser radiation (in addition to relatively high electrical-optical conversion efficiencies) may justify the additional development required. For example, on-board reentry experiments conducted at sizeable source-to-dector distances appear feasible. Although the beam spread of semiconductor lasers is as large as $\pm 10^{o}$ around the emission axis, it may be reduced to a fraction of a degree with suitable optics. The microscopic dimensions of the emission plane (see Fig. 2) provide a point source for collimation optics.

III. ION AND PULSED GAS LASERS

Many laser lines in the ultraviolet, visible, and infrared have been observed in gaseous ion lasers since 1964. The laser lines emanate from ionic transitions stimulated by a gas discharge within a long tube. A review of over 200 ion lines produced by 11 different gases (measured up to March, 1965) is given by Bridges and Chester.[12] Laser action has been observed in singly and multiply-ionized Hg, Ar, Kr, Xe, Ne, C, N, O, I, and Cl. Bridges and Chester also report unpublished work which indicates laser production in Zn, Cd, S, and P. The observed wavelengths cover the spectrum from 2357 A^{o} to 1.05μ.

Ion lasers have been operated both CW and pulsed. Bridges and Chester[12] have achieved 40W pulsed output from Ar II with repetitive 20μs excitation, for an average power output of 100 mW. Bennett et al[12] achieved several hundred watts in pulsed argon, and present commercial capabilities approach this range. Several CW systems using argon and krypton have been marketed in the 1 to 10 watt power range.

Intense ion laser lines span the near ultraviolet and visible spectrum, from 2983 Å (O III) to 1.0923μ (Ar II). The fact that these lines originate from transitions between unperturbed ion energy states precludes the temperature tuning available to solid-state laser mediums. However, many of the lines have sufficient intensity, at least when operated in a pulsed mode, to admit nonlinear interaction with external media.

One of the most important developments in intense short wavelength laser sources for nonlinear optical frequency shifting was the discovery by Heard[14] of lasing action in molecular nitrogen. Leonard and Gerry[15, 16] demonstrated that a pulsed N_2 laser (3371 Å) could be operated with an output of several hundred kilowatts in pulses of ~ 20 ns duration. Shipman[17] developed a low-inductance discharge circuit capable of producing a 2.5 MW pulse of about 4 ns duration in N_2 and a 190 KW pulse of about 1.5 ns duration at 5401 Å in neon. The commercial unit developed from the design of Leonard and Gerry produces an average power of 100 mW at 100 pules/second, with peak power of 100 kW and pulse duration of 10 ns. The width of the output laser line is less than one Angstrom.

Liquid lasers offer promise as future spectroscopic sources of high monochromaticity and intensity.[18] Liquids have exhibited outputs similar

to solid-state lasers (Nd, Ruby) with similar optical pumping techniques but considerably lower thresholds. Outputs of several Joules have been observed, with peak power in the output reaching 10-20 MW even without Q-switching.[18, 19] Intensities have been sufficient to produce second-harmonic output using nonlinear optics.[19] However, a great deal of development remains before liquids achieve the operational status of ruby and neodynium lasers.

Flourescent dye solutions have also been operated as tunable laser sources at power levels which are attractive to spectroscopic applications. Laser action has been obtained throughout the whole 4000 $\mathring{A}$ - 7000 $\mathring{A}$ visible region using strong optical pumping.[20, 21] The output laser wavelength is tunable by varying the organic solute concentration. Laser-pumped dye lasers have produced MW intensities in the visible region which are tunable over small wavelength intervals (up to 400 cm^{-1}) by using an external cavity with a rotatable diffraction grating.[22]

IV. FREQUENCY-DOUBLING AND RAMAN SHIFTING

Nonlinear interaction between an intense laser source and suitable crystals or liquids can lead to generation of second harmonics of the incoming laser light. This means that blue and green lines can be obtained from the red emission of conventional solid-state laser (Nd^+, ruby, etc.) and ultraviolet lines around 2,500 $\mathring{A}$ can be obtained from some ion lasers or by second-harmonic generation from second harmonics of red wavelengths. The intensity is proportional to the square of the input power density, and hence the optical quality of the source beam (coherence, divergence) as well as its total power are dominant factors.

Wang and Racette[23] report a frequency-doubling experiment which is typical of the arrangement used by many experimenters. A ruby laser source at 6943 Å is Q-switched to obtain an instantaneous power P of around 10^7 watts, and this beam is then directed with slight focussing through a crystal of ADP.* Second-harmonic output radiation at 3472 Å is observed, with the conversion efficiency being proportional to P^2 whereas at high power the conversion is proportional to $P^{3/2}$. Wang and Racette[23] present a clear theoretical interpretation of these scaling laws. In their experiments, the maximum conversion efficiency observed was 10% at 20 MW input power, yielding 2 MW of 3472 Å power. Terhune et al[24] used a similar experimental arrangement and observed saturation of the second-harmonic conversion efficiency at about 20%; they also measured 0.05% of the input power as third-harmonic ouput at 2313 Å. F. M. Johnson[25] has achieved megawatt pulses of third-harmonic radiation from a Q-switched ruby by adding second-harmonic radiation from a crystal of ADP to the fundamental in a second ADP crystal.

Many laser sources and nonlinear media have been used for second-harmonic generation. Boyd et al[26] have observed CW second harmonics from a carefully-focussed He-Ne laser, indicating the wide power range amenable to this technique. The advent of new nonlinear media (to be discussed in the following Section) with greatly increased conversion efficiencies and resistance to optical damage at high power levels makes

---

*ADP = ammonium dihydrogen phosphate, available from several sources as a crystal of the highest quality.

second-harmonic generation an attractive method of producing intense laser sources in the 2000 Å - 6000 Å region of the spectrum.

Nonlinear interaction between incoming laser light and a Raman-active material results in coherent output radiation which is shifted in energy by a multiple of the Raman bond energy. The most intense shifted line (up to 30% of the incoming beam) corresponds to the absorption of one vibrational quantum and is referred to as the first Stokes line (S_1). Anti-Stokes shifts (AS_1, AS_2, etc.) to higher energies occur by the addition of the bond energy to the incident photon energy, and these lines are considerably less intense than the corresponding Stokes lines. As many as ten shifted lines have been observed to emanate from Raman-active materials subject to intense laser radiation.

More than 100 coherent lines have been observed from the excitation of more than 30 Raman-active materials.[27] The characteristic vibrational frequencies range from 445 cm^{-1} to 4160 cm^{-1}, and many discrete laser lines can be generated by each intense laser source simply by substitution of different Raman-active materials.

Successful use of Raman-shifted lines in atomic spectroscopy requires coincidence between the optical transition line and the laser output wavelength. One might suppose that, with some 45 Raman-active transitions and several pulsed lasers in the power range of 0.1 MW and up, a good probability would exist of overlap between one or more shifted laser lines and the wavelength of interest.[27, 28] Because of the half-widths of Raman-shifted lines are on the order of 2 to 40 cm^{-1}, any coincidence within this half-width will yield acceptable power densities for most laboratory purposes.

As a test of this hypothesis, 18 atomic cesium transitions were compared with Raman-shifted ruby laser frequencies and shifted ruby second harmonics. Inasmuch as the fundamental ruby wavelength shifts continuously from 6934 Å at 77 °K to 6943 Å at 293 °K, a small amount of wavelength tuning was available for each Raman medium. Twelve of the eighteen cesium lines, ranging from 3347 Å to 8761 Å, were conincident with one or more shifted ruby wavelengths to well within the Raman half-widths. A cross-check of all combinations resulting from 10 strong laser lines (from 3371 Å to 10,610 Å) and 45 Raman-active vibrations (frequency shifts from 216 cm^{-1} to 4155 cm^{-1}, S_1, and AS_1) yields a 94% coverage of the entire wavelength spectrum from 3000 Å to 1.6μ; for most wavelengths in the visible region, several combinations are available which would be suitable for spectroscopic purposes.

The primary advantage of Raman shifting is that the sophistication of post-laser optics is minimized. Most Raman-active substances are inexpensive liquids, e.g. benzene, acetone, carbon tetrachloride, and toluene. In some circumstances it may be possible to place the Raman substance within the laser cavity, thus increasing the net power density passing through the Raman cell. To achieve Raman-shifted second harmonics, it is probably more efficient to first Raman-shift the primary output wavelength and then add the shifted line to the fundamental laser wavelength in a nonlinear medium such as ADP.

V. PARAMETRIC OSCILLATION

Perhaps the most versatile laboratory system for laser line spectroscopy is a parametric oscillator configuration.[29, 30] By using advanced

nonlinear optical mediums[31, 32] such as $Ba_2Na\ Nb_5O_{15}$, tunable outputs in both CW and pulsed modes can be achieved. The tunable frequency interval is centered about wavelength which is twice the input, or "pump", wavelength and covers the approximate range $1.4\lambda_{IN} \lesssim \lambda_{OUT} \lesssim 4\ \lambda_{IN}$. Two particularly promising pumping sources are a pulsed N_2 laser (3371 Å)[16, 17] and a similar neon laser operating at 5401 Å[17]. CW outputs in the visible and near infrared should also be possible using commercially-available ion lasers as pumping sources.

Giordmaine and Miller [29, 33] have reported highly efficient (1%) generation of coherent light output from a $LiNbO_3$ crystal pumped with 5300 Å radiation. The pump light was obtained by second harmonic generation using a Q-switched Nd^+ laser (1.06μ). The $LiNbO_3$ crystal is simply a Fabry-Perot cavity with two flat parallel faces which have dielectric coatings to form a resonance for the generated frequencies. Boyd and Ashkin[34] and Giordmaine and Miller[29] give relations for computing the change in cavity dimensions with temperature. This dimension change shifts the output frequency from ω_o to $\omega_o \pm \delta\omega$, where $\delta\omega$ is a calculable function of temperature. The fundamental frequecny ω_o in the Giordmaine-Miller experiment was 1.06μ, twice the wavelength of the 5300 Å pump light and identical to the original Nd^+ output. Fig. 6 presents their experimental results.*

---

*A recent experiment by J. D. Bjorkholm (Appl. Phys. Lett., 13, 53 (1968)) reports up to 22% conversion efficiency between the pump input power and the tunable signal frequency output. This is accomplished by making the external cavity containing the parametric oscillator resonant to both the signal and idler frequencies.

The previous discussion of parametric oscillation ignores many subtle effects that do not, in practice, allow successful arbitrarily fine tuning of the shifted output wavelength by temperature alone. An electric field must also be applied to the crystal.[34] Furthermore, the nonlinear medium must be transparent at both the pump and output wavelengths.

A similar experiment was conducted by Miller and Nordland[35] in which a $LiNbO_3$ crystal was rotated within an external mirror cavity to achieve tuning. Some advantages accrue to this method of operation; for example, no electric fields need be applied to a constant-temperature crystal. The output power depends exponentially on the inverse of the cavity length and a cavity formed by external mirrors (rather than dielectric-coated crystal faces) runs the risk of inherently lower power outputs.

One of the most important developments in nonlinear optical generation (including the generation of harmonics, frequency mixing, and parametric oscillation) was the discovery of improved nonlinear optical media.[31, 32] The new class of crystal compositions with so-called "filled sites" exhibits significantly increased resistance to optical damage at high average power levels and large nonlinear optical coefficients. Geusic etal[31] report a CW second-harmonic conversion efficiency of nearly 100% using a crystal of $Ba_2Na\ Nb_5O_{15}$ placed within the optical cavity of a Nd:YAG laser operating at 1.06μ, yielding 1.1 W of CW power output at 0.532μ. Previous nonlinear media such as $LiNbO_3$ were not able to sustain such high CW powers without suffering irreversible damage. The nonlinear coefficients of $Ba_2Na\ Nb_5O_{15}$ are roughly 3 times those of $LiNbO_3$. Care must be exercised in choosing parametric oscillator mediums which are compatible with the pump and output wavelengths. Although the nonlinear medium KDP is transparent down to 2800 Å (and hence admits the use of both the 3371 Å N_2 line and the 3472 Å ruby second harmonic), some of the more favorable crystals for optical parametric

oscillation do not transmit at these low pump wavelengths. $Ba_2Na\ Nb_5O_{15}$, for example, is transparent from 4000 Å to 5μ.[31]

Achievement of satisfactory power levels using parametric oscillation essentially gurantees the ability to produce coherent light sources spanning the entire visible and infrared spectrum. The lower wavelength limit depends on the availability of parametric oscillator mediums which are transparent in the near ultraviolet; the ruby third harmonic 2313 Å is readily available as a pump source, and would cover the approximate wavelength interval 3100 Å to 9200 Å.

A different method of generating continuously-tunable laser outputs has been investigated by Carman, Hanus, and Weinberg.[36] The technique relies on the frequency addition of two coherent laser sources in a nonlinear external medium such as KDP. One of the two inputs is the unshifted fundamental of the primary laser source; the second is a (tunable) wavelength interval selected from the broad-band radiation emenating from self-focussing and small-scale trapping of the primary laser beam in a long liquid cell. The method is similar in principle to the addition of fundamental and Raman-shifted beams in a nonlinear medium to produce discrete frequencies near the second harmonic. It differs in that, whereas the Raman-shifted lines are discrete with widths on the order of 2 to 40 cm^{-1}, the small-scale trapping and self-focussing produces a relatively wide continuum band of radiation around the input frequency. In the experiment by Carman, Hanus, and Weinberg,[36] a 30 MW pulsed Nd glass laser was used as the primary source, CS_2 was used as the liquid cell, and KDP

was the final nonlinear mixing medium. The maximum overall conversion efficiency (power is divided by tunable output power) was on the order of 0.03% near the Nd second harmonic of 5300 Å, and dropped to less than 10^{-3}% at wavelengths displaced $\pm$ 480 Å from the second harmonic. This small overall conversion efficiency is unattractive when compared to parametric oscillation or Raman-shifting methods.

VI. APPLICATIONS TO SPECTROSCOPIC DIAGNOSTICS

The characteristic properties of gases- - - temperature, velocity, number density - - - are of crucial concern in many fields of applied physics. Studies of high-temperature gases are continually confronted by measurement problems under severe environmental conditions such as in on-board reentry experiments or in the interior regions of energy conversion and controlled fusion devices. Many standard types of mechanical probes, even if they survive the extreme ambient conditions, perturb the medium being studied and/or are ambiguous in their interpretation. The situation is particularly untenable when it is necessary to obtain very detailed information about the medium with good spatial resolution. In nonequilibrium flows, for example, the number densitites in particular atomic or molecular energy levels may be required. Response time may also be important in some applications, for example shock-produced plasmas.

It is for these reasons that increasingly frequent use has been made of spectroscopic techniques. Although not a panacea in all cases, spectroscopy offers many new possibilities for hitherto unaccessible information.

The interest of this paper, as is evident from the preceding Sections, is in spectroscopic techniques employing optical excitation of selected

energy states of molecules and atoms, and subsequent interpretation of the induced effects on the gas being studied. All of the measurements to be discussed could, in principle, be accomplished with sufficiently intense conventional light sources such as flash tubes or arc sources. Laser sources, however, offer many advantages and often make the difference between a theoretical possibility and a practical experiment.

It is useful to enumerate the advantages which lasers possess in spectroscopic applications. First, the instantaneous power density per unit frequency interval at a particular wavelength is much larger than is available from even the most intense flash tubes. The specifications of one current developmental-type ablating quartz tube[37] are a 5μs half-width, an effective black-body temperature of 30,000 ^{o}K above 2000 $\overset{o}{A}$, an effective collecting area of 0.1 steradians, and a source size of 2.5 mm dia. by 12.7 mm long. This unit produces 2.3 watts/$\overset{o}{A}$ bandwidth at 2000 $\overset{o}{A}$ and 0.072 watts/$\overset{o}{A}$ at 6000 $\overset{o}{A}$. By using one of the several frequency-changing methods discussed previously, it should be possible to produce laser intensitites on the order of 10^2 - 10^3 watts/$\overset{o}{A}$ at any preselected wavelength from about 2500 $\overset{o}{A}$ to several microns, with pulse times ranging from about 10 nanoseconds to a few milliseconds.

Second, the good collimation of laser sources, typically 0.1 radian half-angle divergence or less, allows extremely accurate focussing of the laser beam at substantial distances from the source. Although the effective laser diameter (i.e. the minimum focussed image of the beam) varies with the operating power level, it is generally on the order of a few tenths of a millimeter. Flash-tube and arc sources have effective dimensions roughly ten times as large, hence the instantaneous power densitites achieveable with focussed lasers are much greater.

The final four advantages relate to experimental convenience. The reliability of lasers currently being marketed is quite high, and they are generally much less troublesome than ablating quartz flashtubes in the 30,000 + ^{o}K range. Unwanted radiation is either nonexistent or can be easily filtered out, in contrast to black-body sources which produce a large fraction of their output in uninteresting regions of the spectrum. Further, in the case of CW experiments the intensity of laser sources can be conveniently modulated to allow phase-sensitive detection schemes with enhanced signal-to-noise ratios. And finally, the low intensities and/or high relative levels of background radiation often attendant to flash lamps normally require sophisticated detection systems including high-resolution spectrographs; the higher intensities available from lasers can often obviate the need for spectrographs and allow simpler detection systems.

The use of lasers in resonance scattering experiments can be exemplified by the following generalized procedure. Laser light is focussed into the volume of gas to be studied, and photons are absorbed by one or more particular atomic or molecular excitation transitions. The population densities of the initial and final states of the absorption transitions are altered, thereby influencing the amount of line radiation emanating from the effected volume of gas. Observations are made of the intensities and profiles of one of more emisssion lines by external optics focussed on the test volume. By using appropriate theoretical and/or empirical interpretations, it is possible to deduce local properties of the gas such as number density, velocity, and temperature.

A system of the type described above was used by Hoffman[38] and others[39-42] to determine the ion density in barium plasmas. Hoffman's excitation source was the bright continuum of a mercury capillary arc rather than a laser, but in other respects the arrangement was identical to that described previously. The singly-ionized alkaline earths are particularly well suited to flourescent scattering because they possess strong resonance absorption lines in the visible region. Excitations of the $6^2S_{1/2}$ ground state of Ba^+ to the first two excited P-levels, $6^2P_{3/2}$ and $6^2P_{1/2}$, occur at 4554.0 $\mathring{A}$ and 4934.1 $\mathring{A}$ respectively. For the experimental conditions of Hoffman, deexcitation of the two 6P levels occurred primarily by re-radiation to the ground state, and consequently by measuring the intensity ratio of incident exciting light to light reradiated at 90^o, it was possible to determine the ion density. This experiment was performed in a strong magnetic field and Zeeman splitting and anisotropic reradiation of the 4934.1 $\mathring{A}$ line was observed. Resonance radiation of Ba^+ at 4554.0 $\mathring{A}$ is always unpolarized and isotropic, independent of the magnetic field and the direction and polarization of the incident light source.

Hoffman's experiment represents a point measurement of the number density of absorbing Ba^+ ions. A similar technique can be used to measure neutral atom densities of alkali metals because they also possess electronic transitions corresponding to photon energies in the visible spectrum. For example, the ground state to first excited state resonance transitions in neutral cesium correspond to 8944 $\mathring{A}$ and 8921 $\mathring{A}$. The low-lying states of Ba^+ and Cs^o are illustrated in Fig. 7.

It is possible to deduce the temperature of the species by repeating the measurement for two different optical transitions. For Ba^+, for example,

repeating the relative intensity measurement using excitation of the 5854 Å transition $5D_{3/2} \rightarrow 6P_{3/2}$ and monitoring subsequent reradiation at 4554 Å one could obtain the population of the $5D_{3/2}$ level. The species temperature T would then be given by the Boltzmann equation

$$N_k/N_j = (g_k/g_i) \exp - (E_k-E_j)/kT$$

where (E_k-E_j) is the energy difference between two states, $N_{k,j}$ are the population densities of the states, and $g_{k,j}$ are the state degeneracies. Additional accuracy can be obtained by measuring several excited-level densities and verifying that a Boltzmann relation holds between the states. It should be possible to "seed" gases with alkalis or other species to allow measurement of local temperatures and densities in otherwise inaccessible situations. The only additional assumption (beyond those inherent in interpreting the induced spectroscopic signal[38]) is equilibrium between the spectroscopic "seed" atoms and the parent gas.

The importance of laser excitation, even for self-luminous gases, becomes self-evident when it is recognized that the optical signal received by an external detector is integrated over the entire cone of view intercepting the gas. By preferentially exciting one small volume element within this viewing path it is possible to relate the differential signal to the local properties of the excited volume.

Muntz[43, 44] has developed a very successful electron-beam flourescence technique which is quite similar to the laser flourescence method. In both schemes the gas volume coincident to both the exciting beam and the receiver optics is the local point at which measurements are made. The primary limitation to laser excitation is that the pumping transition must

have an energy difference within the capability of existing lasers and shifted laser lines, i.e. ΔE less than about 6eV. Electron-beam techniques have other limitations such as excitation of many unwanted levels and poor coupling between the beam energy and the particular transitions which one wishes to excite. The ranges of atoms and molecules and their densities and temperatures amenable to electron-beam excitation and optical excitation are not necessarily coincident.

Interpretation of the line profiles of laser-induced optical emission provides additional information on the local temperature and particle densities of a gas. The spectral line emanating from an atomic electronic transition is broadened by the natural lifetimes of the excited states, the thermal and directed Doppler motion of the atoms, and collisional interactions between the radiating particle and other atoms and charged particles. Natural broadening is normally small compared to thermal and collisional effects.

Wiese[45] has summarized current line-broadening theories which include charged particle neutral (Stark) collisions. For dilute gases with low ionization, thermal Doppler broadening dominates and the line half-width is easily related to the translational temperature of the gas. However, Doppler half-widths are quite small, on the order of 0.001 to 1 $\text{\AA}$ in high-temperature laboratory plasmas. A most successful instrument for measuring this narrow profile is a Fabry-Petrot etalon.[44] In cases where the gas motion has a mean velocity component parallel to the direction of observation, an absolute measurement of the Doppler shift of the line center will yield a measurement of the gas velocity. However, this method of velocity determination is quite difficult in practice because it is necessary to

make an absolute calibration of wavelength. Destructive interference can be used to accomplish this by beating the shifted wavelength against the primary laser beam.

In plasmas, radiative transitions originating from or terminating in states far removed from the ground state are subject to significant Stark broadening from neutral-charged particle collisions. Both electrons and ions contribute to Stark broadening, but in essentially different regions of the profile.[45, 46] Under certain conditions[45] Stark broadening either dominates the emission line profile or can be extracted from a combination of Doppler and Stark effects. Using tabulated theoretical values for Stark broadening[46] it is possible to determine the electron density from the Stark-broadened half-width. Only a rough estimate of the electron temperature is required to make this calculation. However, the accuracy of the plasma density measurement is no more accurate than the theoretical values of the Stark parameters, and hence the minimum uncertainty ranges from around 20% for some hydrogenic lines to more than a factor of two for more complicated atoms.

Once again the measurement of line profiles enhanced by laser pumping of excited states allows point measurements within the gas. For self-luminous gases, without such enhancement, the best one can hope for is radial symmetry and an Abel inversion via a series of measurements at different radii. Radiation from gases which are known a priori to be uniform do not require anything more than integrated measurements. Uniformity allows many other spectroscopic techniques which are presently in widespread use (c.f. Regs. 45-49). Some progress has recently been reported

in interpreting line-reversal measurements of temperature in nonuniform alkali plasma,[50] but the interpretation of line radiation from non-uniform self-luminous gases is difficult at best. A large body of astrophysical literature is devoted to this subject.

Flourescence techniques in molecular gases are considerably more difficult to interpret because of the large number of states which can be excited by the light source. The broader the half-width of the exciting source, the larger the number of transitions which are excited. The monochromaticity and high intensity of lasers has made possible a large number of molecular flourescence studies of diverse types. Representative results are reported in Refs. 51-56.

Tango, Link, and Zare[56] performed an experiment in which laser excitation of K_2 flourescence was accomplished using the 6328 $\mathring{A}$ line of a He-Ne laser. The laser, with a line width of 0.05 cm^{-1}, populated upwards of 5 rotational-vibrational levels of the electronically-excited $B^1\pi_u$ state of the K_2 molecule. Subsequent flourescent radiation returned the molecule to the ground electronic state, and the rotational band structure of the emission was interpreted to yield precise values for the potential function of the ground state. In some cases, a study of the flourescent spectrum can also yield information on collisional energy transfer rates.[45, 55]

Of more direct application to diagnostic experiments is the excitation of the so-called γ band of transitions in NO which connect the electronically-excited $A^2\Sigma^+$ state with the $X^2\pi$ ground state.[57] These optically-allowed transitions represent energies in the vicinity of 2200 $\mathring{A}$. Typical calculations of LTE line absorption coefficients are given by Golden[58], and are

reproduced in Fig. 8. Provided that the natural lifetimes of the excited electronic states are short compared to the time for collisional depopulation, the ratio of incident to flourescent light intensity represents a direct local measure of the population density in the particular NO vibrational state excited by the incident radiation.

A similar experiment appears feasible in O_2 which is highly excited in vibration. The Schumann-Runge transitions which connect the $X^3\Sigma^-_g$ ground state with the $B^3\Sigma^-_u$ electronically excited molecule comprise a well-known system with relatively high absorption. The energy difference between the ground vibrational levels of these two states is 6.120 eV, or slightly more than the electronic ground-state dissociation energy of 5.080 eV. There are no selection rules governing the change of vibrational quantum number during the electronic transition; the intensity of emission and absorption is determined by the Franck-Condon overlap between pairs of vibrational levels, one in each electronic configuration. Golden[58] has calculated the absorption of the Schumann-Runge system of O_2 based upon an equilibrium population distribution of vibrational levels in the $X^3\Sigma^-_g$, ground state, and the result for T = 2000 ^oK is given in Fig. 9.

The Schumann-Runge absorption of O_2 is negligible at low temperatures because the highest transition probabilities (i.e. most favorable Franck-Condon overlaps) coincide with the upper vibrational levels of the electronic ground state, and the population densitites of the upper vibrational levels are, in equilibrium, proportional to exp-[E ($\nu>o$) - E($\nu=o$)]/kT. At temperatures of several thousand degrees, however, the population densities in the upper vibrational levels are sufficient to make flourescent

scattering using lasers a feasible diagnostic technique. Furthermore, the photon energy required to excite the upper vibrational levels of $X^3\Sigma_g^-$ to the corresponding vibrational levels of $B^3\Sigma_u^-$ is considerably less than the energy difference between the two vibrational ground states. For a ground-state vibrational quantum number $v = 5$, the energy difference is about 5.5 eV, and for $v = 15$ the required excitation energy has dropped to around 3.4 eV. These photon energies are well within the state-of-the-art of high-intensity lasers, particularly the 3371 $\mathring{A}$ N_2 molecular line[17] and the 2313 $\mathring{A}$ ruby third harmonic.[25] Furthermore, at elevated temperatures the absorption curve of O_2 is nearly continuous (see Fig. 9) so that no fine tuning of the laser frequency is required. Resonance emission may be considerably weakened by the tendency of the $B^3\Sigma_u^-$ state to undergo non-radiative autodissociation or collisonal dissociation.[59]

The previous examples of the use of resonance flourescence in gas temperature and density measurements is far from exhaustive, but suggests the possibilities inherent in current laser capabilities. Collisional depopulation of electronically-excited states can often make the interpretation of flourescent intensities ambiguous, and in molecular flourescence in particular there may be great difficulty in assigning accurate values to the branching ratios for competing radiative deexcitation paths. A similar problem in the electron-beam excitation of nitrogen and argon was overcome by empirical calibration[43, 60, 61], and this is a distinct possibility for laser-induced flourescence as well.

Velocity measurements in flowing gases can also be accomplished using laser flourescence techniques. At some initial time the laser is focussed into the gas and a small volume is excited to upper electronic states from which it subsequently decays. Provided the characteristic spontaneous emission lifetime τ is long compared to the time required for the excited volume to move downstream a distance equal to its own diameter, the flourescence can be tracked in time and the velocity of the particle trajectory determined. Streak photographs or an image-converter camera may be used, as tracking detectors.

Two modes of excitation should be distinguished. One is "massive excitation," and by this it is meant that the laser intensity is sufficiently high to cause localized electrical breakdown at the focus of the beam. The techniques for producing such sparks in air have been studied in a number of laboratories, and are reviewed by Meyerand.[62, 63] The resulting plasma is highly ionized and its self-expansion is not negligible. The actual distribution of energy among the various degrees of freedom of the gas has not been resolved, but the optical emission contains the electronic recombination continuum, atomic recombination continuum, and line radiation from electronic deexcitation.[64]

Rittenhouse[65] and his collaborators have succeeded in making accurate velocity measurements by this method in a high-enthalpy supersonic stream of air. The conditions of this experiment were $M_\infty \approx 1.7$, $T_\infty \approx 5000\ ^\circ K$, p_∞ = 1 atmosphere, and the velocity on the order of 2000 m/sec. Excitation was accomplished with a focussed Q-spoiled ruby laser of 150 MW power. The minimum electric field strength required for breakdown[62] is approximately proportional to $p^{-2/3}$ below one atmosphere, and massive excitation becomes impractical at low densities.

The second method involves selective excitation of atomic or molecular electronic states using laser line radiation. Using the data of Keck etal[66] and Allen,[67] it is possible to estimate the absorption of common molecular bands observed in N_2, O_2, and NO. For velocities on the order of 2,000 - 4,000 in/sec., it is necessary to excite transitions with natural radiative lifetimes on the order of 10^{-5} to 10^{-6} sec. in order to have sufficient intensity to optically track the trajectory of the excited gas. Sample calculations were performed for air travelling at 3600 m/sec. with a vibrational temperature of 2000 ^{o}K and a total density of 0.4×10^{-2} atmos. Measurement of the flourescence of the NO(γ) band ($B^2\pi \rightarrow X^2\pi$) excited by the ruby third harmonic at 2314 $\mathring{A}$ should yield accurate velocity measurements provided that the initial diameter of the excited column of gas at the focus is less than 0.1 cm and the ruby third harmonic power is greater than 1 MW.

REFERENCES

1. B. A. Lengyel, Introduction to Laser Physics, Wiley, N. Y., 1966, esp. Chs. III and V.

2. H. F. Ivey, IEEE J. Quantum Electronics, QE-2, 713 (1966).

3. F. F. Morehead, Jr., Scientific American, Vol. 216, pp. 109-122, May, 1967. The efficiencies quoted in this article may be somewhat optimistic but are indicative of what may be practical in the near future.

4. These data are taken from specifications for RCA Developmental Type TA 2628 (Dec., 1966) for a single emitting element plus corroborating information from the same laboratory appearing in the literature (see M. F. Lamorte et. al., IEEE J. Quant. Elect., QE-2, 9 (1966)). These half-widths are considerably less than those reported by other investigators at equivalent temperatures (B. A. Lengyel, Ref. 1, p. 145). Diode arrays consisting of a number of independent lasing elements in series have considerably larger half-widths, on the order of 40-50 Å. Presumably proper quality control can reduce the array bandwidth to that of a single element.

5. M. Garfinkel and W. E. Engler, IEEE Solid State Devices Research Conference, Michigan State U., 1963.

6. M. Lax, Science, 141, 1247 (1963).

7. C. Hurwitz, Appl. Phys. Lett., 8, 243 (1966).

8. C. Hurwitz, Appl. Phys. Lett., 8, 121 (1966).

9. F. H. Nicol, Appl. Phys. Lett., 9, 13 (1966).

10. T. Gonda, H. Junker, and M. F. Lamorte, IEEE J. Quantum Elec., 1, 159 (1965).

11. C. Hurwitz, Appl. Phys. Lett., 9, 116 (1966).

12. W. B. Bridges and A. N. Chester, IEEE J. Quantum Electronics, 1, 66 (1965)

13. W. R. Bonnett Jr., J. W. Knutson, Jr., G. N. Mercer, and J. L. Detch, Appl. Phys. Lett., 4, 180 (1964).

14. H. Heard, Nature, 200, 667 (1963)

15. D. A. Leonard, Appl. Phys. Lett., 7, 4 (1965)

16. E. T. Gerry, Appl. Phys. Lett., 7, 6 (1965)

17. J. D. Shipman, Jr., Appl. Phys. Lett., 10, 3 (1967)

18. A. Heller, Physics Today, Nov., 1967, p. 35.

19. A. P. Lempicki and H. Samuelson, Sci. Am., 216, 81 (1967).

20. P. P. Sorokin, J. R. Lankard, E. C. Hammond, and V. L. Moruzzi, IBM J. Res. Dev. 11, 147 (1967)

21. S. C. Claesson and L. Lindquist, Kemi, 12, 1 (1958) Y. Miyazoe and M. Maeda, Appl. Phys. Lett., 12, 206 (1968).

22. H. B. Soffer and B. B. McFarland, Appl. Phys. Lett., 10, 266 (1967).

23. C. C. Wang and C. W. Racette, J. Appl. Phys., 36, 3281 (1965).

24. R. W. Terhune, P. D. Maker, and C. M. Savage, Appl. Phys. Lett., 2, 54 (1963)

25. F. M. Johnson, private communication to Dr. J. Hall, Joint Institute for Laboratory Astrophysics, Boulder, Colo.

26. G. D. Boyd etal., Phys. Rev., 137, A1305 (1965)

27. G. Eckhardt, IEEE J. Quantum Elect., QE-2, 1 (1966)

28. S. Yoshikawa and Y. Matsumura, Appl. Phys. Lett., 8, 27 (1966)

29. J. A. Giordmaine and R. C. Miller, Appl. Phys. Lett., 9, 298 (1966).

30. R. C. Miller and W. A. Nordland, Appl. Phys. Lett., 10, 53 (1967)

31. J. E. Geusic etal, Appl. Phys. Lett., 11, 269 (1967) and 12, 306 (1968).

32. K. F. Hulme etal, Appl. Phys. Lett., 10, 133 (1967)

33. J. A. Giordmaine and R. C. Miller, Phys. Rev. Lett., 14, 973 (1965). See also Physics of Quantum Electronics, P. L. Kelly etal (Eds.), Mc Graw-Hill, N. Y., 1966, pp. 31-42.

34. G. D. Boyd and A. Ashkin, Phys. Rev., 146, 187 (1966)

35. R. C. Miller and W. A. Nordland, Appl. Phys. Lett., 10, 53 (1967)

36. R. L. Carman, J. Hanus, and D. L. Weinberg, Appl. Phys. Lett., 11, 250 (1967).

37. Dr. S. Mastrup, TRW Systems, Inc., private communication.

38. F. W. Hoffman, Phys. Fluids, 7, 532 (1964)

39. N. Rynn, E. Hinnov, and L. C. Johnson, Phys. Fluids, 8, 1368 (1965)

40. M. Hashmi, A. J. Vander Houren van Oordt, and J. G. Wegrove, in Proc. Conf. on Physics of Quiescent Plasmas, Vol, II, Laboratori Gas Ionizzati, Frascati, 1967, pp. 523-530.

41. R. O. Motz, I. C. Rogers, and A. D. Bates, in Proc. Conf. on Physics of Quiescent Plasmas, Vol. II, Laboratori Gas Ionizzati, Frascati, 1967, pp. 531-542

42. E. Hinnov etal, Phys. Fluids, 6, 1779 (1963)

43. E. P. Muntz, Phys. Fluids, 5, 80 (1962)

44. E. P. Muntz, Phys. Fluids, 11, 64 (1968)

45. W. L. Wiese, in Plasma Diagnostic Techniques, R. L. Huddlestone and S. L. Leonard (Eds.), Academic Press, N. Y., 1965, pp. 265-317.

46. H. R. Griem, Plasma Spectroscopy, McGraw-Hill, N. Y. 1964.

47. R. L. Huddlestone and S. L. Leonard (Eds.), Plasma Diagnostic Techniques, Academic Press, N. Y., 1965. See esp. Chs. 5, 6, 8, 9, and 10.

48. A. C. G. Mitchell and M. W. Zemansky, Resonance Radiation and Excited Atoms, 2nd Ed., Cambridge, U. Press, London and New York, 1961.

49. W. K. McGregor, in Physio-Chemical Diagnostics of Plasmas, Northwestern U. Press, Evanston, 1963, pp. 143-166.

50. G. Brederlow, and R. T. Hodgson AlAA J., 6, 1277 (1968)

51. W. B. Tiffany, H. W. Moos, and A. L. Schawlow, Science, 157, 40 (1967)

52. J. R. Novak and M. W. Windsor, J. Chem. Phys., 47, 3075 (1967)

53. K. G. P. Sulzmann, F. Bien, and S. S. Penner, J. Quant. Spectros, and Rad. Trans., 7, 969 (1967)

54. A. M. Ronn, J. Chem. Phys., 48, 511 (1968)

55. J. T. Yardley and C. B. Moore, J. Chem. Phys., 48, 14 (1968)

56. W. J. Tango, J. K. Link, and R. N. Zare, J. Chem. Physics (in Press)

57. M. Jeunehomme, TRW Systems, Redondo Beach, Calif., private communication. For additional features of the NO - γ bands, see M. Jeunehomme, J. Chem. Phys., 45, 4433 (1966)

58. S. A. Golden, J. Quant. Spectros, Rad. Trans., 7, 225 (1967)

59. T. W. Bond, Jr., K. M. Watson, and J. A. Welch, Jr., Atomic Theory of Gas Dynamics, Addison - Wesley, Reading, Mass., 1965, p. 165.

60. S. L. Petrie, The Ohio State University, ARL Report 65-122 (1965).

61. F. Robben and L. Talbot, Institute of Engineering Research Report AS-65-4, University of California, Berkley (1965).

62. R. G. Meyerand, Jr. "Laser Plasma Production - A New Aera of Plasmadynamics Research," AlAA Paper No. 66-174, March, 1966.

63. A. F. Haught, R. G. Meyerand, Jr., and D. C. Smith, in Physics of Quantum Electronics, McGraw-Hill, New York (1966), p. 509.

64. E. Archibold, D. W. Harper, and T. P. Hughes, Brit. J. Appl. Phys., 15, 1321 (1964)

65. L. Rittenhouse, AEDC, Tullahoma, Tenn., private communication.

66. J. C. Keck, R. A. Allen, and R. L. Taylor, J. Quant. Spectros. Rad. Trans., 3, 335 (1963).

67. R. A. Allen, "Air Radiation Tables: Spectral Distribution Functions for Molecular Band Systems," AVCO Research Report 236, April, 1966.

FIGURE CAPTIONS

1. Schematic of Current-Injection Laser.

2. Schematic of Electron-Beam Pumped Semiconductor.

3. Semiconductor Compounds Exhibiting Laser Action. (Solid Lines indicate that the production of intermediate wavelengths has been observed; dashed lines indicate that a portion of the spectrum has been observed or that laser action is probable.

4. Wavelengths of $CdSxSe_{1-x}$. (From C. Hurwitz, Appl. Phys. Lett., 8, 243 (1966)).

5. Resolution of a Typical Output Line from ZnS. (From C. Hurwitz, Appl. Phys. Lett., 9, 116 (1966)).

6. Continuous Generation of Line Radiation Between 0.73μ and 1.93μ by Optical Parametric Oscillation. (From Giordmaine and Miller, Appl. Phys. Lett., 9, 298 (1966)).

7. Typical Spectroscopic Lines Arising from the Alkali Earths and Metals (a) Low-lying energy levels of Ba^+. (b) Low-lying energy levels of Cs.

8. Absorption Coefficient of the $NO(A^2\Sigma^+ - X^2\pi)$ γ - Band System at 2000 °K. [After S. A. Golden, J. Quant. Spectros. Rad. Tr., 7, 225 (1967)].

9. Absorption Coefficient for the $O_2(B^3\Sigma_u^- - X^3\Sigma_g^-)$ Schumann-Runge Band System at 2000 °K. [After S. Golden, J. Quant. Spectros. Rad. Tr., 7, 225 (1967)].

ACKNOWLEDGEMENTS

This investigation was supported by the Atomic Energy Commission (Contract AT-(11-1)-1776) and the Air Force Flight Dynamics Laboratory (Contract F 33615-67-C-1850). The initial stimulation for this investigation arose at the Institut für Plasmaphysik, Garching, Germany, during a 1966-67 Faculty Fellowship from the University of Colorado. I wish to thank Dr. G. Von Gierke of the Institute für Plasmaphysik for his encouragement during this period. The critical comments of Dr. Jan Hall of the Joint Institute for Laboratory Astrophysics, Boulder, were also extremely valuable.

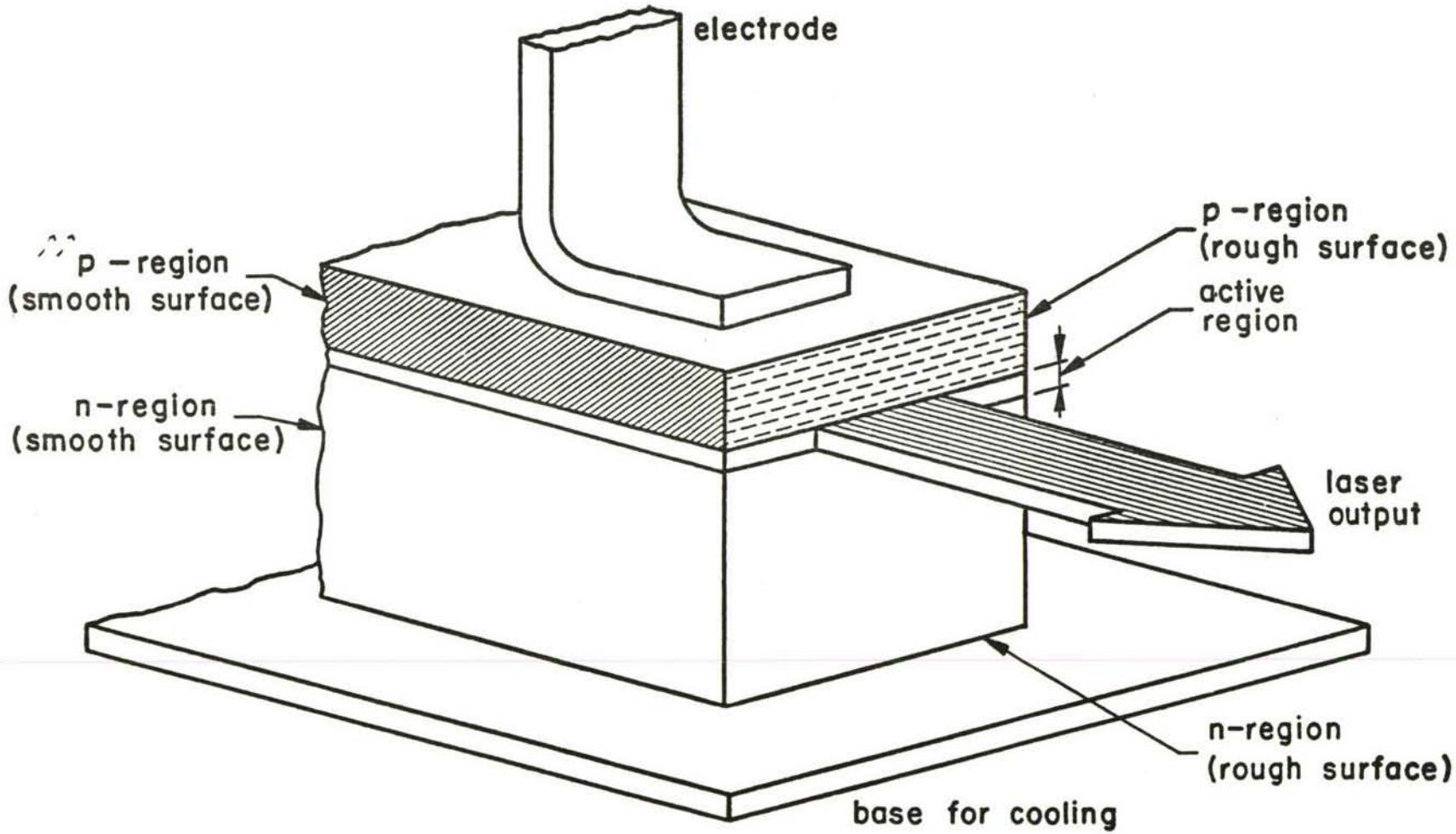
electrode
p -region
(rough surface)
p -region
(smooth surface)
active
region
n-region
(smooth surface)
laser
output
n-region
(rough surface)
base for cooling

FIGURE 1

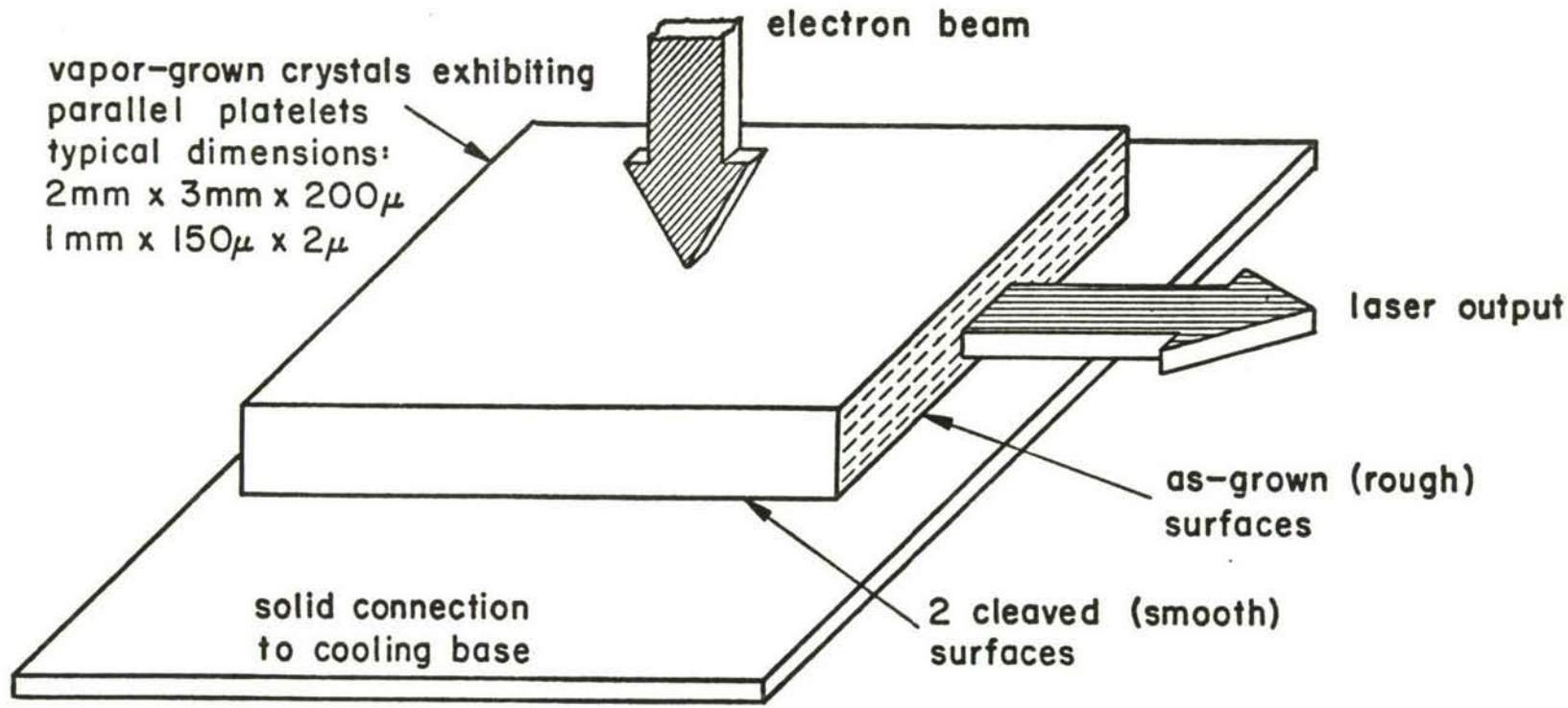
electron beam
vapor-grown crystals exhibiting
parallel platelets
typical dimensions:
2mm x 3mm x 200μ
1mm x 150μ x 2μ
laser output
as-grown (rough)
surfaces
solid connection
to cooling base
2 cleaved (smooth)
surfaces

FIGURE 2

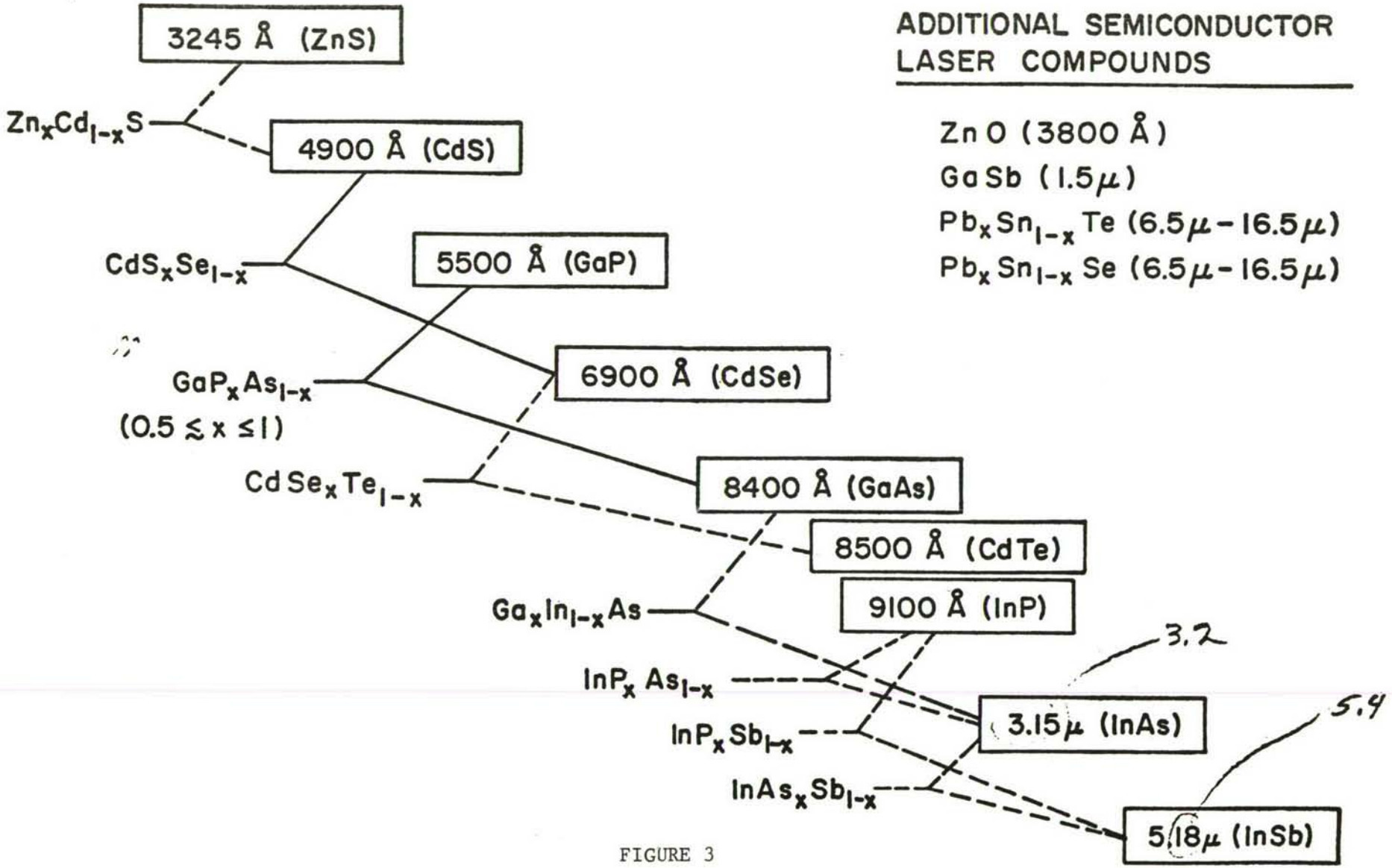

ADDITIONAL SEMICONDUCTOR LASER COMPOUNDS

ZnO (3800 Å)
GaSb (1.5μ)
$Pb_xSn_{1-x}Te$ (6.5μ - 16.5μ)
$Pb_xSn_{1-x}Se$ (6.5μ - 16.5μ)

FIGURE 3

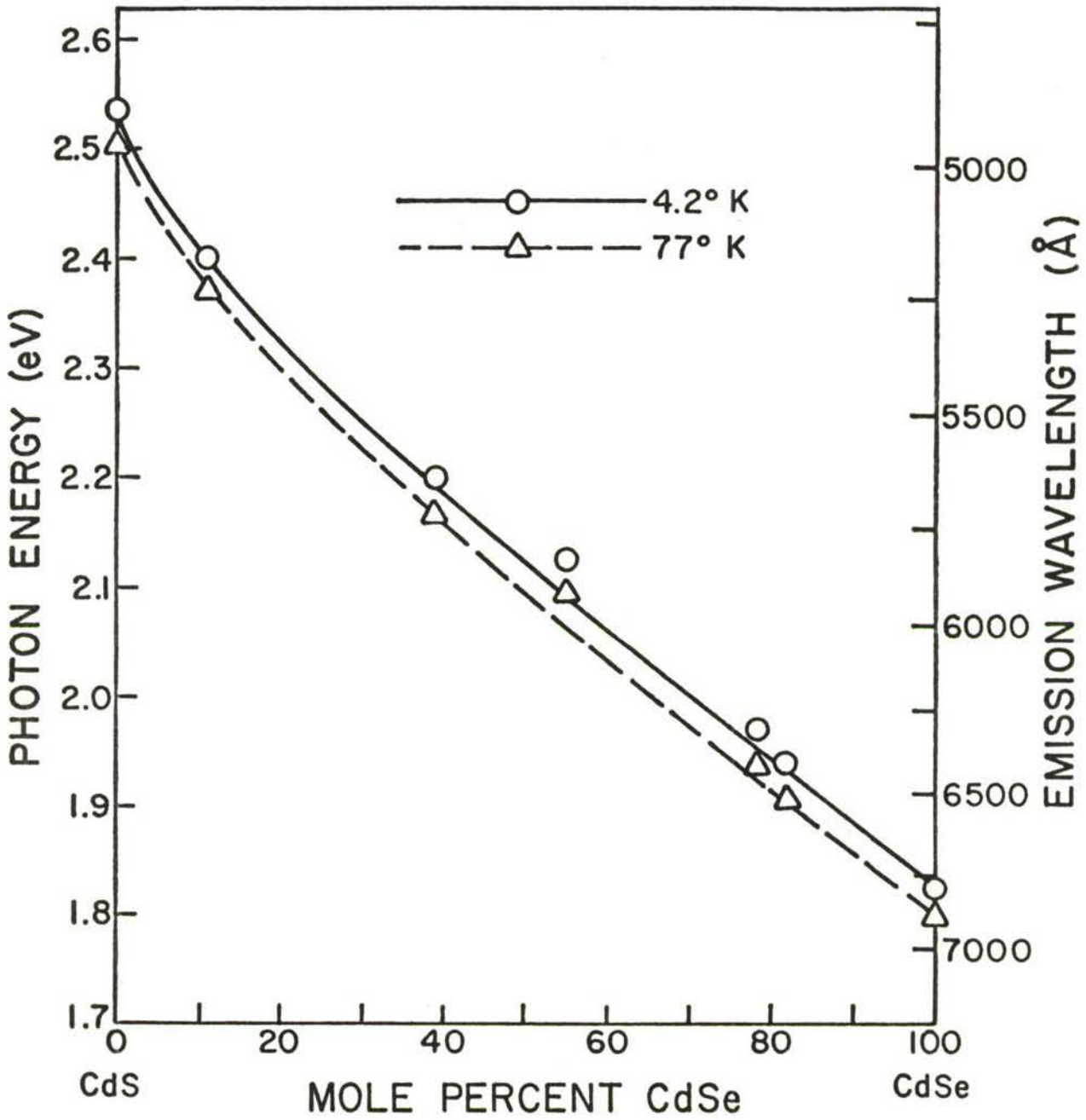
2.6
2.5
2.4
2.3
2.2
2.1
2.0
1.9
1.8
1.7
PHOTON ENERGY (eV)
4.2° K
77° K
5000
5500
6000
6500
7000
EMISSION WAVELENGTH (Å)
0
20
40
60
80
100
CdS
MOLE PERCENT CdSe
CdSe

FIGURE 4

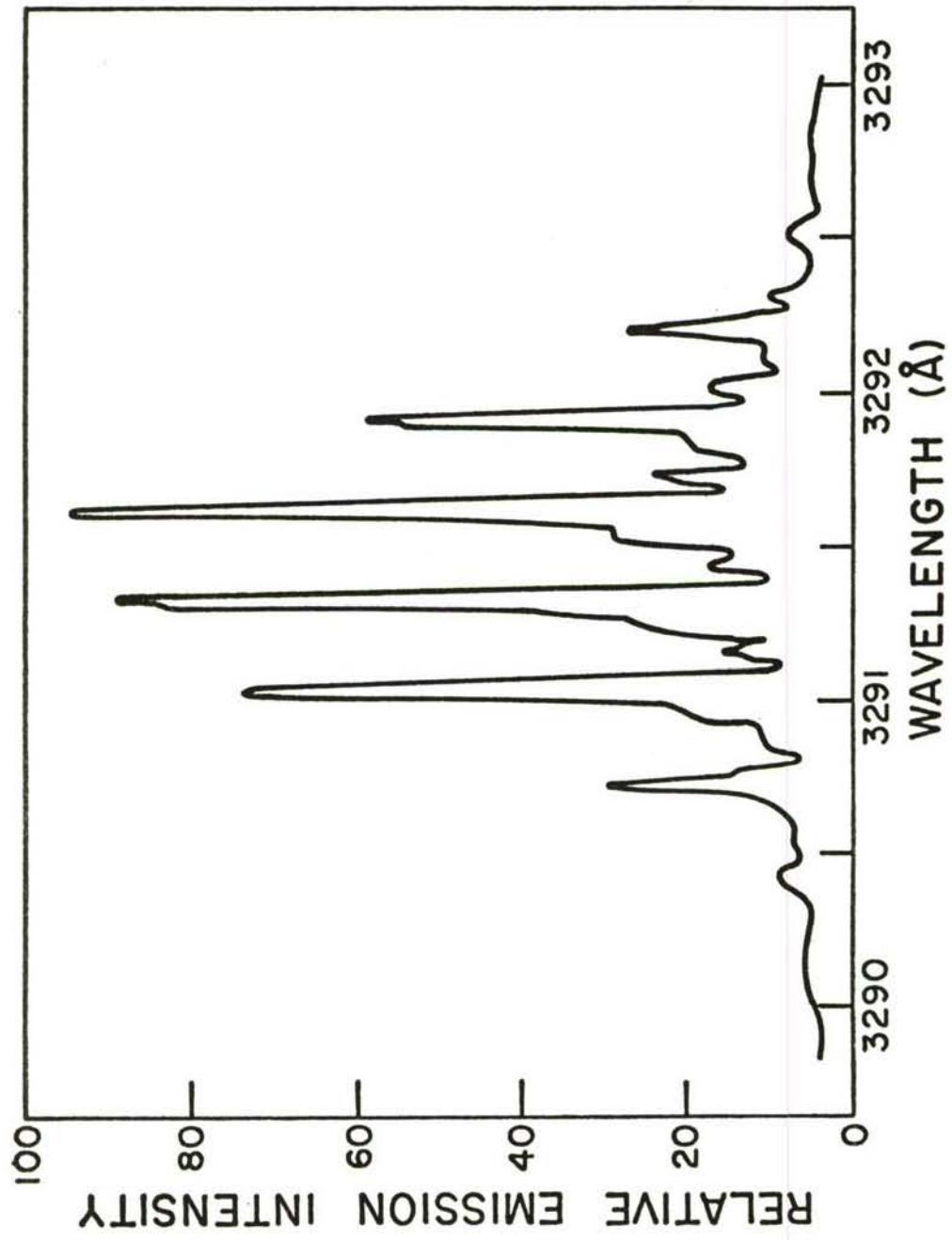
RELATIVE EMISSION INTENSITY
100
80
60
40
20
0
3290
3291
3292
3293
WAVELENGTH (Å)

FIGURE 5

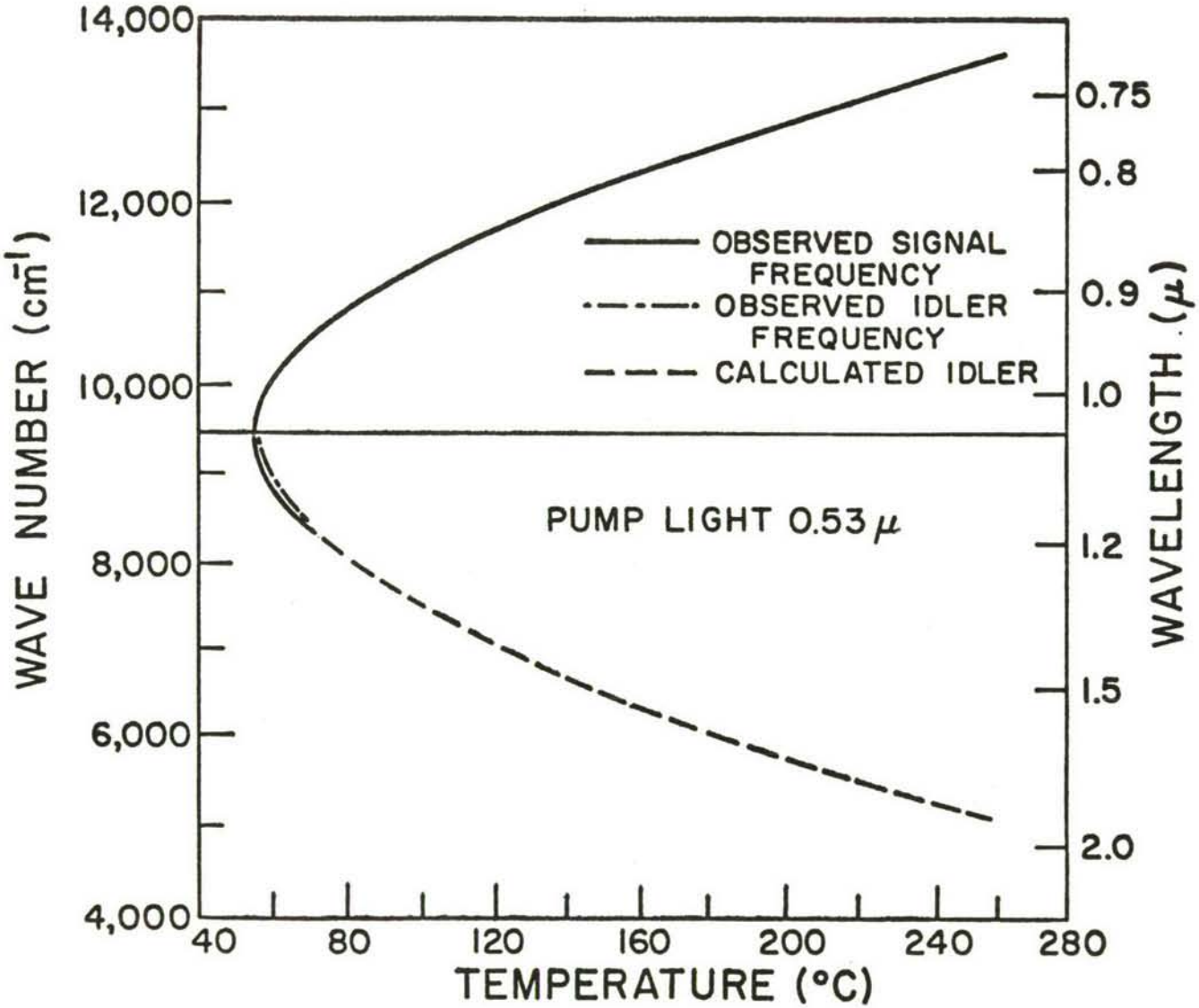
14,000
12,000
10,000
8,000
6,000
4,000
WAVE NUMBER (cm⁻¹)
0.75
0.8
0.9
1.0
1.2
1.5
2.0
WAVELENGTH (μ)
OBSERVED SIGNAL FREQUENCY
OBSERVED IDLER FREQUENCY
CALCULATED IDLER
PUMP LIGHT 0.53 μ
40
80
120
160
200
240
280
TEMPERATURE (°C)

FIGURE 6

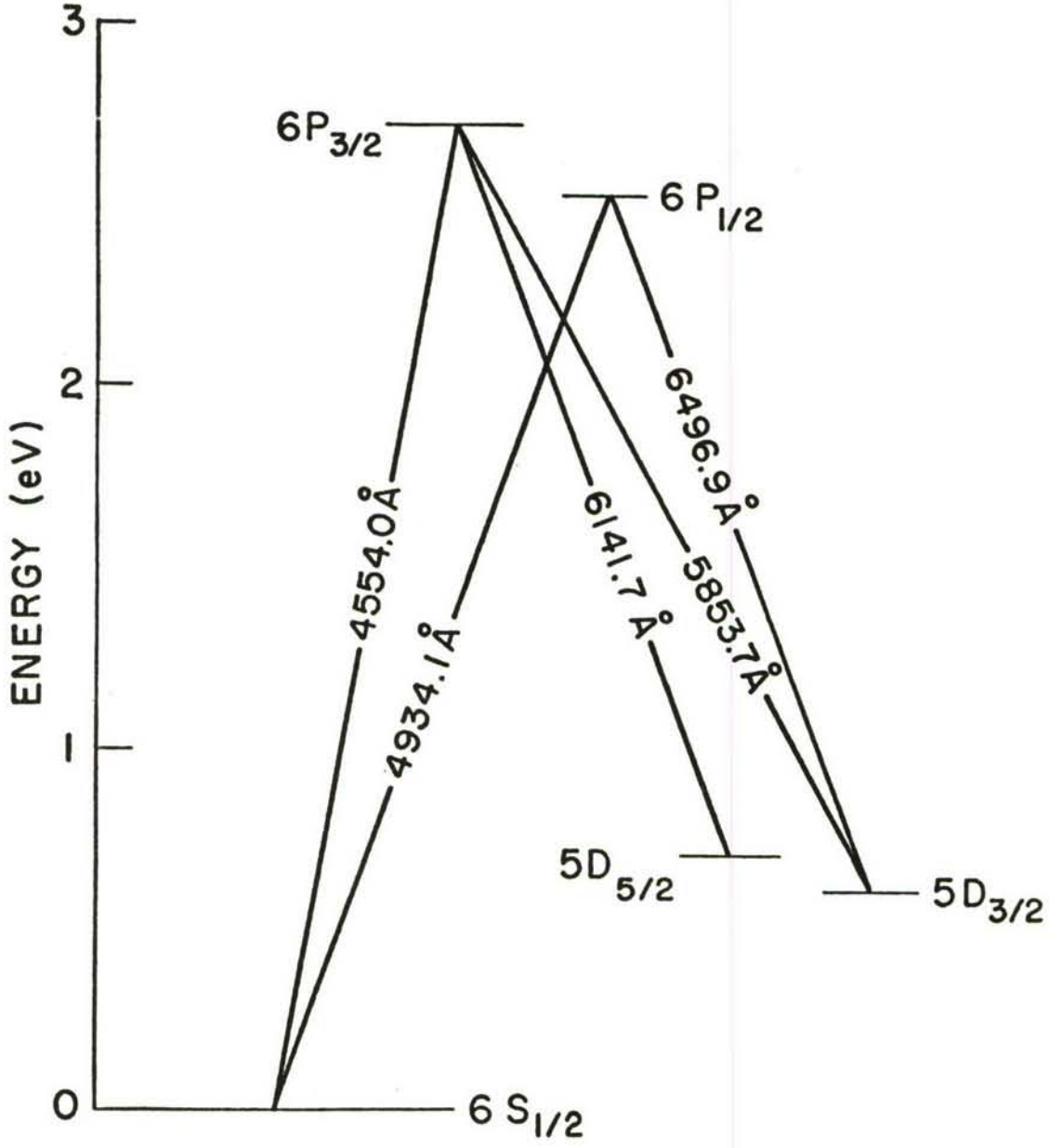
3
2
1
0
ENERGY (eV)
6P3/2
6 P1/2
4554.0Å
4934.1Å
6141.7 Å
6496.9Å
5853.7Å
5D5/2
5D3/2
6 S1/2

FIGURE 7a

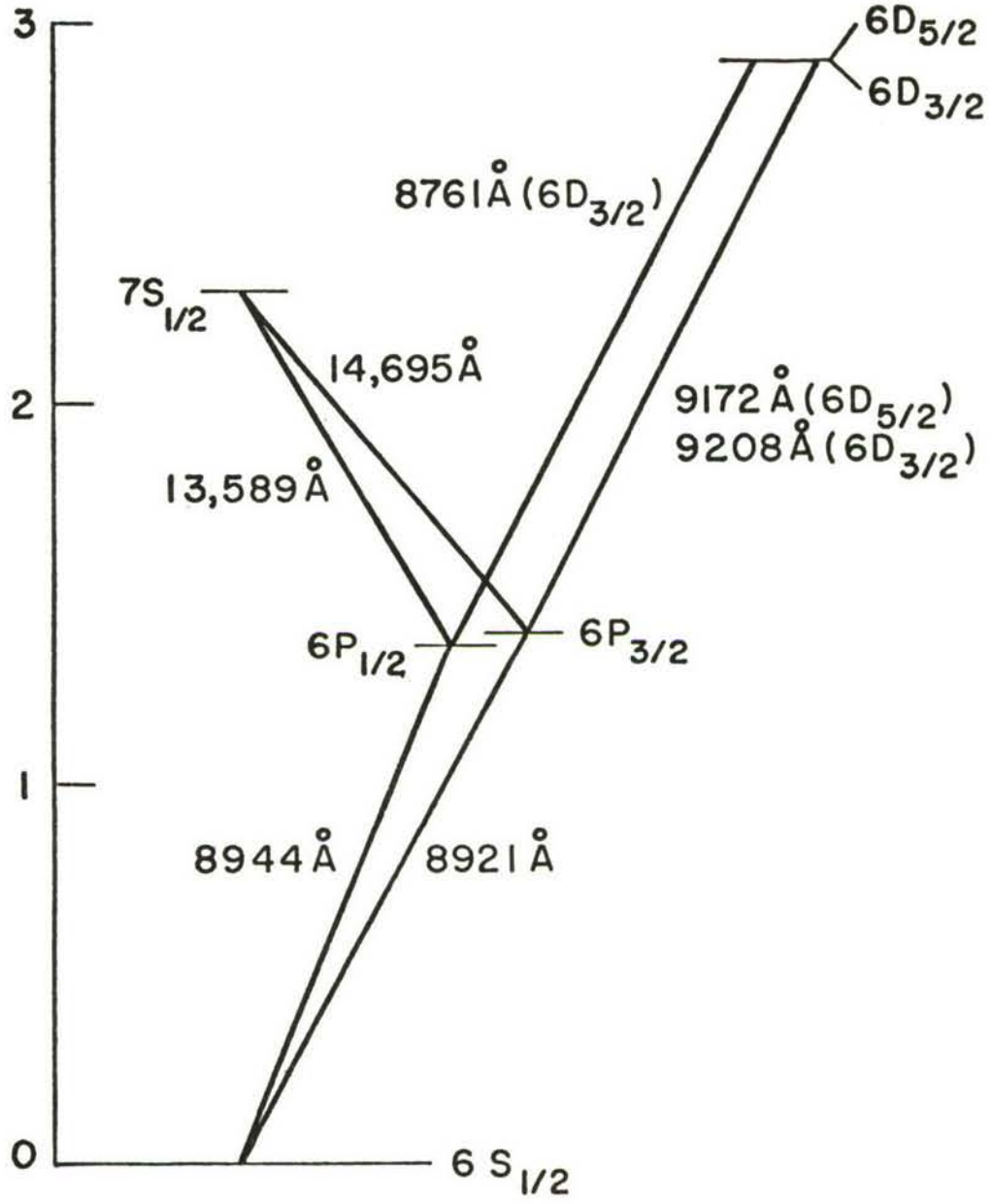
3
2
1
0
6D5/2
6D3/2
8761Å (6D3/2)
7S1/2
14,695Å
9172 Å (6D5/2)
9208Å (6D3/2)
13,589Å
6P1/2
6P3/2
8944Å
8921 Å
6 S1/2

FIGURE 7b

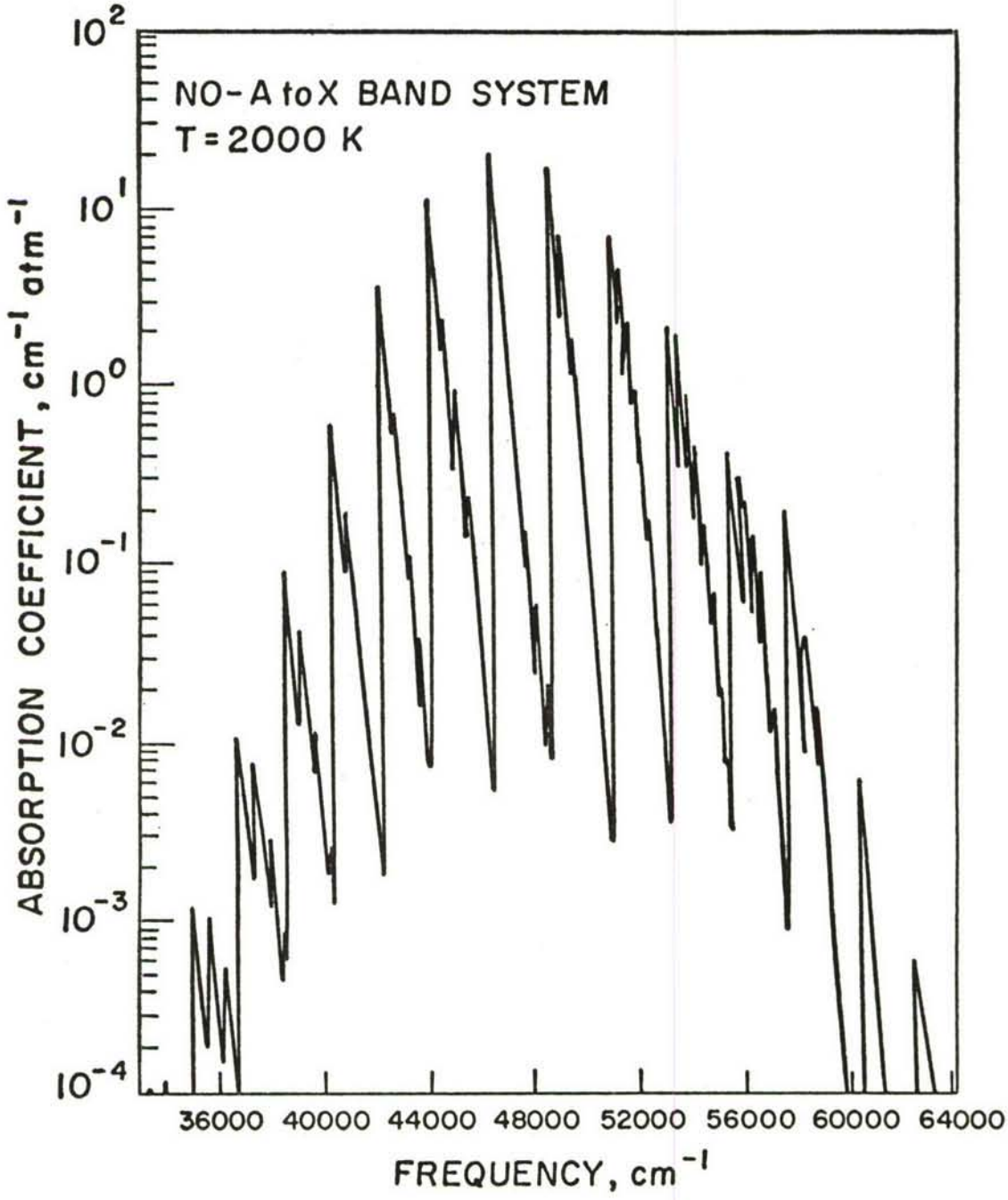
NO-A to X BAND SYSTEM
T = 2000 K
ABSORPTION COEFFICIENT, cm⁻¹ atm⁻¹
10²
10¹
10⁰
10⁻¹
10⁻²
10⁻³
10⁻⁴
36000 40000 44000 48000 52000 56000 60000 64000
FREQUENCY, cm⁻¹

FIGURE 8

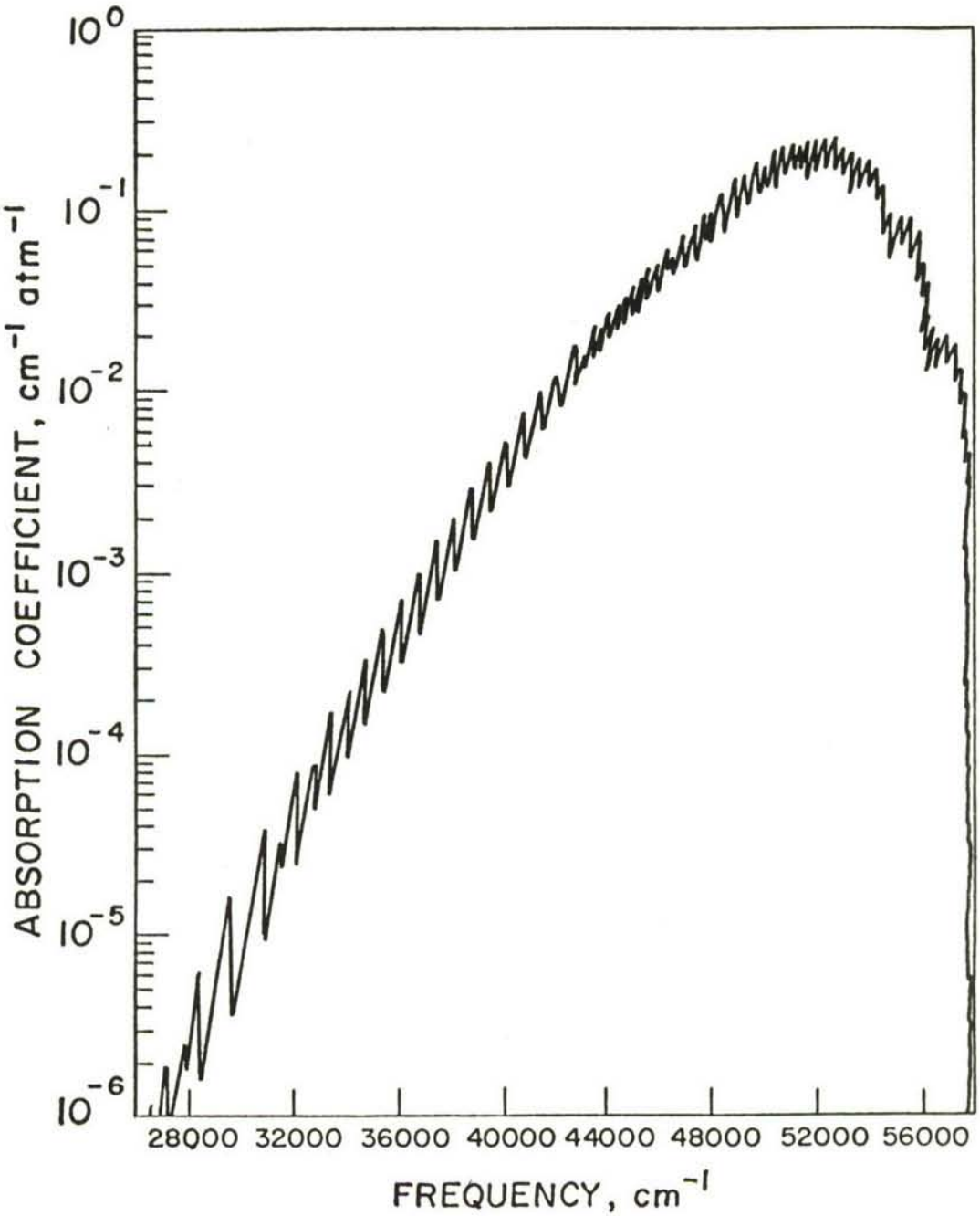
ABSORPTION COEFFICIENT, cm⁻¹ atm⁻¹
10⁰
10⁻¹
10⁻²
10⁻³
10⁻⁴
10⁻⁵
10⁻⁶
28000 32000 36000 40000 44000 48000 52000 56000
FREQUENCY, cm⁻¹

FIGURE 9

ATTACHMENT B

VOLUME IONIZATION VIA LASER RADIATION IN A CESIUM PLASMA DIODE

by

C. Forbes Dewey, Jr.*
University of Colorado, Boulder, Colorado

and

Peter E. Oettinger**
Joint Institute for Laboratory Astrophysics
University of Colorado, Boulder, Colorado

ABSTRACT

This paper considers the possibility of enhancing neutralization of the interelectrode space charge in a cesium diode by the use of line radiation. Ionization results from a two-step process. The neutral cesium atoms are first raised to an excited electronic level by line radiation (typically from a solid-state laser).

---

*Present address: Department of Mechanical Engineering, Massachusetts Institute of Technology, Cambridge, Mass.

**Present address: Plasma Research Laboratory, Aerospace Corporation, El Segundo, California.

The excited neutrals, being within a few kT of the continuum, are then collisionally ionized by plasma electrons. A detailed consideration of the optical excitation cross-sections and electron-neutral collision cross-sections for the highly-excited states suggests that plasma densities of 10^{15} cm^{-3} can be produced. The thermal economics of this system appear to be attractive when compared to contact ionization and collisional ionization as well as previously proposed schemes employing radiation.

I. INTRODUCTION

The basic physical mechanisms controlling the behavior of cesium plasma diodes operating in the gas discharge or "ignited mode" appear to be understood.[1] Although some controversy surrounds the detailed ionization and recombination events within the diode[1-4], the primary features of the experimental current-voltage (I - V) curves agree qualitatively with the postulated mechanisms[5]. In the most interesting I - V regions, ionization occurs via collisions between neutral Cs atoms and electrons, the latter having an elevated temperature by virtue of being injected into the plasma across the electrostatic sheath adjoining the emitter surface. The resulting ions are necessary to cancel the electron space charge in the main plasma of the interelectrode gap.

This Introduction begins with a review of the limitations on diode performance when ion production occurs via contact ionization and volume ionization. Subsequent sections examine the possibility of achieving enhanced plasma densities by photo-excitation of neutral cesium.

A. Contact and Volume Ionization

Contact ionization has been used for many years to produce ions from low ionization potential gases such as cesium. The

ionization probability P of an incoming ion or neutral is given by the Saha-Langmuir relation

$$P = (1 + \nu_o / \nu_i)^{-1} \qquad (1)$$

where

$$(\nu_o / \nu_i) = \text{(neutral evaporation rate)/(ion evaporation rate)}$$

$$= (g_o/g_i) \exp - (e\Phi_w - E_i)/kT \qquad (2)$$

where g_o and g_i are the state degeneracies of the neutral species and the corresponding ion, Φ_w is the effective surface work function[6], and E_i the ionization potential. For a high ionization probability, the work function must be large compared to the Cs ionization potential of 3.893 eV.

A second relation defining electron emission from a surface at temperature T_s is the Richardson-Dushman equation

$$j_s = 120.2\ T^2 \exp - (e\Phi_w/kT_s),\ \text{amp/cm}^2 \qquad (3)$$

where T is in ^oK. As $e\Phi_w$ increases and therefore P becomes significant, the electron saturation current j_s drops to an unacceptably small value; conversely, as $e\Phi$ decreases to a minimum (less than 2 eV for cesiated surfaces), contact ionization becomes inefficient because P becomes smaller than 10^{-4}. Compounding this difficulty

is the fact that the emitter sheath often acts to reduce this ion flux from the surface by a large factor, say 10^2 to 10^4, by reflecting surface-generated ions back to the emitter[7-10].

The second ionization source, and the one which dominates ignited-mode operation of thermionic converters, is collisional ionization. Three possible mechanisms have been suggested for this mode: (a) direct collisional ionization of Cs atoms from the ground state; (b) two-step processes forming molecular ions; and (c) multi-step collisional ionization forming atomic ions.

Collisional ionization of the ground-state atom can be represented by

$$Cs(6S_{1/2}) + e + 3.893\ eV \rightarrow Cs^+ + e \qquad (4)$$

The recent data of Heil and Scott[11] report a maximum cross-section for the removal of the 6S electron of about 5.5×10^{-16} cm^2 at 10 eV, rising roughly parabolically to this value from threshold, while Nygaard[12] reports a higher cross-section near threshold.

Two-step ionization[2,13] to form Cs_2^+ is described by the reaction

$$Cs(6S_{1/2}) + e + \begin{Bmatrix} 1.386\ eV \\ 1.455\ eV \end{Bmatrix} \rightarrow \begin{Bmatrix} Cs(6P_{1/2}) \\ Cs(6P_{3/2}) \end{Bmatrix} + e \qquad (5)$$

$$Cs(6P) + Cs(6P) + (?)\ eV \rightarrow Cs_2^+ + e \qquad (6)$$

The dissociation energy of Cs_2 is 0.46 eV and the ionization potential of Cs_2 is assumed to be 3.28 eV by Harris[13] so that the formation of unexcited Cs_2^+ from two ground-state Cs atoms requires 2.82 eV. The collisional energy in Eq. (6) therefore lies between +0.05 eV if the two excited states are Cs ($6P_{1/2}$) and -0.09 eV for a collision of two Cs ($6P_{3/2}$) atoms. Witting and Gyftopoulos[2] estimate that the cross-section for formation of Cs_2^+ from two excited atoms is extremely large, on the order of 1450×10^{-16} cm^2, and hence the rate-controlling step in this reaction is the formation of Cs (6P) according to Eq. (5)[14]. Their estimate of the excitation cross-section for Cs ($6S_{1/2}$) → Cs ($6P_{1/2,3/2}$) is based on the semi-classical impact parameter method and rises from threshold to a maximum of 95×10^{-16} cm^2 at 7 eV. It should be noted that the rate of formation of Cs_2^+ according to Eq. (6) depends on the square of the density of excited states, and hence will be extremely limited if either the excited state density or the cross-section for the reaction of Eq. (6) is small. Furthermore, the two-body dissociative recombination of Cs_2^+ and e by the formation of excited molecules will be extremely fast; the life-time for highly-excited Cs_2 is on the order of 10^{-13} sec.[15] Wilkins[16] has demonstrated that the concentration of Cs_2^+ is important only for plasma densities $N_e < 10^{12}$ $cm.^{-3}$

The third ionization mechanism, the formation of atomic ions by multiple collisions, involves a multiplicity of excitation steps of the form

$$Cs\ (\text{state } k') + M \rightarrow Cs\ (\text{state } k'') + M \qquad (7)$$

where M may be an electron, a ground-state or excited atom, or an ion. A common observation in related problems (e.g. the ionization rate of argon behind a shock wave in a shock tube[17]) is that the rate-controlling step is the excitation of ground-state atoms to the first few excited levels via electron-neutral collisions. This is particularly true when the electron temperature exceeds the atom temperature (as it normally does in practical thermionic converters) and electron collisions dominate the transitions between upper levels.

Consequently, for electron densities above 10^{12} cm^{-3} and temperatures below one electron volt, it is generally believed that (1) molecular ions represent only a small fraction of the ions present in the ignited mode[14,18,19], and (2) the formation of atomic ions via one-step electron collisions appears to be improbable if the injected electrons from the emitter are Maxwellized. (This is probably the reason that in the so-called "quasi-saturation" region[1],

the predominant ion production is found to occur near the emitter[20,21], before the injected electrons have had a chance to thermalize.)

Multi-step processes, while much more difficult to unscramble, are primarily controlled by electron-neutral collisions[22]. An energy level diagram for cesium is given in Fig. 1. It indicates that the first few excited levels are separated by several times the mean electron energy of a converter diode operating in the ignited mode whereas the higher excited states are much more closely spaced and would be expected to have population densities in Saha equilibrium with the free electrons. Therefore, recombination (and hence ionization) depends upon the rate at which transitions occur between the higher levels, in equilibrium with the free electrons, and the lower levels, which tend to equilibrate with the ground state. Both radiative and collisional transitions must be considered. Calculations of this type for cesium have been carried out by Moizhes, Basht, and Melikiya[23], Byron, Stabler and Bortz[24], Dugan, Lyman, and Albers[25], Norcross[21], Zgorzelski[26], Bates, Kingston, and McWhirter[27], and others.

B. Plasma Resistivity Effects

Inherent in the collisional ionization process is a severe penalty in converter output voltage attributable to electron-neutral collisions. As a first approximation, the electrical resistivity

can be decomposed into two independent contributions, one arising from electron-neutral collisions and the second from coulomb interactions. A lower limit for the resistivity can be obtained by neglecting coulomb collisions and is

$$\rho_{min} = \frac{m_e}{e^2} \frac{\sigma_o \bar{v}_e}{N_e/N_o}$$

where σ_o is the cross-section for collisions between electrons and ground-state atoms, $\bar{v}_e$ is the mean electron thermal velocity $(8kT_e/\pi m_e)^{1/2}$, e is the elementary charge, and N_e/N_o is the ratio of electron density to ground-state density. (We assume that nearly all neutrals are in the ground state.) The voltage drop across a uniform plasma of thickness d would then be

$$V_p = e j_e \rho d \qquad (9)$$

where j_e is the electron particle current density. Defining the random electron flux as

$$j_r = \frac{1}{4} N_e \bar{v}_e$$

and combining Eqs. (8) and (9), a lower estimate of the plasma voltage drop is

$$\left(\frac{e V_p}{k T_e}\right)_{min} = \frac{2}{\pi} (\sigma_o d N_o) (j_e/j_r) \qquad (10)$$

Eq. (10) is very useful in that it expresses the plasma loss in terms of parameters which are easily measured or estimated. The current ratio (j_e/j_r) should be maximized for efficient diode performance, but if it exceeds approximately 0.1 the electrons are highly non-Maxwellian and the meaning of T_e becomes ambiguous. Warner and Hansen[28] have summarized the available data for σ_o, and a value of approximately 2.0×10^{-14} cm^2 applies throughout the range of T_e of interest. Using these values, a converter spacing of 0.05 cm, and a neutral density of 2×10^{16} cm^{-3} ($\sim$ 1 Torr),

$$(eV_p/kT_e)_{min} \sim 1.3$$

which represents a plasma power loss of the same order of magnitude as the output power of the diode. At 10 Torr the electron-neutral resistivity loss would be intolerable.

Note that this resistive drop places an upper limit on the allowed neutral density for efficient converter performance. If one assumes σ_o and (j_e/j_r) to be roughly independent of the electron density and eV_p to be of the same order of magnitude as kT_e, then this upper limit for N_o is independent of the plasma

electron density and output current. This implies an inherent limitation to the useful output current if collisional multi-step ionization by thermalized electrons is the only mechanism which sustains the plasma density. To be sure, there is a certain latitude in the establishment of elevated electron temperatures by virtue of particular emitter sheath configurations; but the fundamental limitation on maximum useful output power remains.

C. A Preliminary Description of Laser - Sustained Plasmas

We now inquire into the possibility of sustaining useful plasma densities by "pumping" the plasma with resonance radiation from a laser. As an illustrative model (to be refined later in this paper), we assume that ion losses arise wholly from recombination. Collisional-radiative theory suggests that above some particular levels the number densities in the excited states are in equilibrium with the free electron density at the electron temperature T_e according to the Saha equation

$$\underline{k \geq s} \qquad N_k(N_e,T_e) = 2.06 \times 10^{-16} g_k N_e^2 T_e^{-3/2} \exp(E_I - E_k)/kT_e \qquad (11)$$

where N_k is the density of the k^{th} state, N_e is the plasma electron density, g_k is the state degeneracy, and $(E_I - E_k)$ is

the difference between the ionization potential E_I and the energy of the k^{th} level. In Eq. (11), the densities are in units of cm^{-3} and the temperature is in ^{o}K.

Without further elaboration of the detailed radiative and collisional processes leading to recombination, we can form a qualitative picture of the state population distributions N_k for the conventional "ignited mode" operation and for a plasma "pumped" with line radiation. This is illustrated in Fig. 2. If the lower states are in equilibrium with the ground-state density N_o and determined by electron-neutral collisions, then the density distribution would be given by the Boltzmann equation:

$$N_k(N_o, T_e) = N_o\left(\frac{g_k}{g_o}\right) \exp - (E_k/kT_e) \qquad (12)$$

In practical diodes, the distribution may differ from Eq. (12) because of untrapped line radiation[18,24-27]. Although intense radiation from the doublet transitions $(6P_{1/2}, 6P_{3/2}) \rightarrow 6S_{1/2}$ is highly trapped even for plasma thickness on the order of 10^{-2} cm, a significant fraction of the radiation arising from transitions which end in excited states escapes from the plasma.

Now consider the possibility of "pumping" the plasma with intense line radiation corresponding to some particular excitation

$k' \rightarrow k''$ from a level $k' < s$ to a level $k'' > s$ which is in equilibrium with the free electron density according to Eq. (11). Because of the large rate of upward excitations produced by pumping, both the equilibrium recombination rate and the free electron density exceed the values sustained solely by collisional processes. The finely-dashed curve of Fig. 2 suggests the distribution which would be expected if both optical pumping and collisional ionization are employed.

The free electron density depends of course on the intensity of the incoming radiation. A simple model of this relationship, to be refined in subsequent sections, can be constructed by neglecting radiative decay and assuming that the net excitation rate must equal the net recombination rate which is proportional to the frequency of electron collisions with atoms in the lowest state which is in equilibrium with the electron continuum [$k = s$ in Eq. (11)]. Then

$$\begin{aligned} \text{Optical Excitation Rate} &\equiv -\frac{dN_e}{dt} \alpha N_e N_s \bar{v}_e \bar{\sigma}_s \\ &\alpha N_e^3 \bar{\sigma}_s T_e^{-1} \exp(E_I - E_s)/k'T_e \quad (13) \end{aligned}$$

where $\bar{\sigma}_s$ is an appropriately-averaged collision cross-section for all transitions from the s-level to lower states. $\bar{\sigma}_s$ is usually dominated by one or two particular transitions because the individual

cross-sections are approximately proportional to the oscillator strengths of the corresponding optical transitions.

From Eq. (13) we deduce that optical pumping applied to energy conversion devices has an intrinsic upper limit where the power required to drive the optical pumping source is equal to the output power of the device. Inasmuch as the electrical output is roughly proportional to N_e, the fraction of output power required for pumping increases approximately as N_e^2.

II. PHOTOPRODUCTION OF EXCITED STATES

There is sufficient reason to believe that appreciable ionization of cesium atoms can be achieved by a combination of photoexcitation and collisional processes[29,30,31]. In fact, laser radiation from presently available sources could be utilized to increase the ion density in a cesium diode without increasing the neutral atom density, and consequently the contribution of electron-neutral collisions to plasma resistivity.

The efficiency of the optical pumping scheme depends sensitively on the wavelength of the incident radiation. The transition $k' \rightarrow k''$ selected as the excitation step must meet three requirements. First, the oscillator strength $f_{Lu} = f(k' \cdot\cdot k'')$

must be sufficiently large to provide appreciable absorption of the pumping radiation across the thickness of the plasma. (Multiple passes or the placement of the diode within a laser cavity are possible but the optical complexity of the system is increased.) On the other hand, if the absorption occurs in a distance small compared to the plasma thickness the pumping radiation will be primarily absorbed at the plasma boundary without causing significant ionization within the main interelectrode region.

A second requirement is that the pumping transition $k' \rightarrow k''$ be the inverse of the recombination process, i.e., the initial and final states must satisfy $k' < s$ and $k'' > s$. For typical cesium diode conditions this means that the initial level k' is limited to the ground-state ($6S_{1/2}$) or the first group of excited levels ($6P_{1/2}, 6P_{3/2}, 5D_{3/2}, 5D_{5/2}$) and the final state k'' must be roughly within several kT_e of the continuum[24].

The third restriction is that the excitation line be broad enough to trap a significant fraction of the incident radiation. In general the line widths of laser radiation range from a few tenths of an Angstrom to several $\mathring{A}$. The only broadening mechanism producing such large line widths in a diode plasma is Stark broadening from electron-neutral collisions.

A. Absorption Coefficients and Line Profiles.

Consider a specific cesium atom electronic transition represented by a spectral line profile broadened by the natural lifetimes of the excited states, the thermal Doppler motion of the atoms, and collisional interactions between atoms and charged particles. The volume absorption coefficient k_{ν_o} at the line center is

$$k_{\nu_o} = k_o \exp\left[\left(\frac{\Delta\nu_N + \Delta\nu_C}{\Delta\nu_D}\right)^2 \ln 2\right] \operatorname{erfc}\left[\frac{\Delta\nu_N + \Delta\nu_C}{\Delta\nu_D} (\ln 2)^{1/2}\right] \quad (14)$$

where the constant k_o and the thermal and Stark half-widths[32] are functions of the line center frequency ν_o, the atom and electron masses m_a and m_e, and the temperatures T_e and T_a. These relations are[33,34]

$$k_o = \frac{2}{\Delta\nu_D} (\pi \ln 2)^{1/2} \frac{e^2}{m_e c} N_L f_{Lu} \quad (15)$$

$$\Delta\nu_D = \frac{2\nu_o}{c} \left(\frac{2kT_a \ln 2}{m_a}\right)^{1/2} \quad (16)$$

$$\Delta\nu_C \approx \frac{2wN_e c}{10^{24}\lambda_o^2}\left[1 + 1.75\,\alpha\left(\frac{N_e}{10^{16}}\right)^{1/4}\left(1-0.75r\right)\right] \quad (17)$$

where for singly-charged ions

$$r = 6^{1/3}\pi^{1/6}\left(\frac{e^2}{kT_e}\right)^{1/2} N_e^{1/6} \quad (18)$$

The quantities α and w are slowly-varying functions of temperature and have been tabulated by Griem[33].

The natural half-width $\Delta\nu_N$ of a line is determined by the lifetimes of excited atoms. It is normally small compared to the thermal or Stark widths in a plasma. However, a strong radiation field can cause a substantial increase in stimulated emission thereby enhancing the natural half-width. Our preliminary calculations suggest that for conditions relevant to laser-pumped thermionic converters, $\Delta\nu_N$ will be small compared to $\Delta\nu_C$ and can be neglected in Eq. (14).

Incident radiation of specific intensity I_{ν_o} is absorbed along its path direction according to

$$-\frac{dI_{\nu_o}}{dx} = I_{\nu_o}(x)k_{\nu_o}(x) \quad (19)$$

For resonance transitions involving the first excited states k_{ν_o} is large enough, under normal operating conditions of the diode, to

readily absorb any incoming radiation of wavelength ν_o near the plasma boundaries. Consequently, in order to increase the penetration of this radiation more deeply into the plasma the Stark half-width $\Delta\nu_C$ of the line must be increased.

In fact, when the thermal broadening of a line becomes negligible with respect to the Stark width, the resultant absorption coefficient profile $k_\nu(\nu)$ is approximated by a Lorentzian function, and the absorption, at a distance x in from the boundaries of a uniform plasma, of a beam of incoming radiation with constant specific intensity I_o can be expressed in terms of an equivalent line width W as[35]

$$W = \int_o^\infty \frac{I_o - I_\nu}{I_o} \, d_\nu = \frac{\pi e^2 N_L f_{Lu} x}{m_e c} \, e^{-Ax} \left[J_0(iAx) - iJ_1(iAx) \right] \qquad (20)$$

where J_0 and J_1 represent Bessel functions of the zeroth and first order, and the constant A is defined as

$$A = \frac{e^2 N_L f_{Lu}}{m_e c \, \Delta\nu_C}$$

Differentiating Eq. (20) with respect to the Stark half-width $\Delta\nu_C$ shows that an increase in this half-width results in an increase

in the total absorption of radiation by the plasma. Therefore, as long as the absorption line width is narrower than an incoming beam of constant specific intensity an increase in the Stark broadening (with all other parameters kept constant) increases both the total radiation energy absorbed by a uniform plasma and the penetration depth into the plasma of energies near the line center.

The most accurate f-values for cesium are to be found in the definitive paper by Stone[36], and the broadening calculations have been experimentally verified by Stone and Agnew[37]. For cases where the transition line width is small compared to the exciting laser line width, Eq. (20) applies and the details of the profile are important only insofar as different parts of the profile will be absorbed in different parts of the diode. If the two line widths are comparable, then an accurate "folding" of the two lines must be made to determine the absorption per unit volume in various parts of the interelectrode region. Uniform volume absorption should not be anticipated in practical diodes, even for weakly-absorbed lines, because the electron density and hence the state populations N_k from Eq. (11) varies across the plasma[37,38].

B. Favorable Excitation Transitions

The details of collisional-radiative recombination theory and substantiating experiments can be found in References 15, 18,

21 - 27, and 39. A detailed calculation of the excited state density distribution N_k with strong laser pumping is beyond the scope of this paper, but the general features exhibited by previous collisional-radiative calculations should apply.

The first order of business is to estimate the term value s above which the state populations $N_k(T_e, N_e)$, $k \geq s$, are in equilibrium with the free electrons according to the Saha equation, Eq. (11). There is ample evidence[2,18,25] to show that the resonance radiation from the transitions $6P_{1/2} \rightarrow 6S_{1/2}$ and $6P_{3/2} \rightarrow 6S_{1/2}$ is effectively trapped within the diode and that the two 6P states are in Boltzmann equilibrium with the $6S_{1/2}$ ground state according to Eq. (12). Moizhes et al[23] have demonstrated that the two 5D levels are in Boltzmann equilibrium with the 6P levels and, therefore, the first four excited state densities follow Eq. (12). By similar arguments, it may be inferred that the state quartets 7P - 6D, 8P - 7D, etc. have relative Boltzmann populations within each group, but it does not follow that the quartets are in equilibrium with one another.

Aleskovskii[40] has examined the afterglow of a decaying cesium plasma, for conditions very similar to what one would expect in a plasma pumped with laser radiation. He concluded that

the primary contributions to recombination come from 4F - 5D and 6D - 6P transitions (see Fig. 1). Because of the large deexcitation rate from the 4F and 6D levels, the population densities of these states should be somewhat below the Saha densities of Eq. (11). All higher levels, however, should be close to equilibrium with the free electron density because the spacing between adjacent levels is of the order of kT_e or less.

In summary, the levels 6P and 5D are in equilibrium with the ground-state density according to Eq. (12). The levels 8S and 8P and above are nearly in equilibrium with the continuum according to Eq. (11), whereas the densities in the 7S, 7P, 6D, and 4F levels are intermediate to these two descriptions. In addition, the quartet of levels 7P - 6D are in Boltzmann equilibrium with each other. The term value for s corresponds (approximately) to the $8P_{1/2}$ level.

Favorable laser-induced transitions satisfying $k' < s$ and $k'' > s$ would include the following series:

6S → 8P, 9P, ---

6P → 7D, 8D, ---

5D → 5F, 6F, ---

Table 1 lists pertinent data on these series plus other transitions of possible interest in judging partial LTE between levels. Electron-

neutral inelastic cross-sections for collisional transitions scale roughly as the f-numbers for corresponding optical transitions.

C. Calculations for Specific Transitions

One may neglect the contribution of ion-neutral collisions to the Stark half-width without any significant loss of accuracy for diode calculations. Then the dimensional forms of Eqs. (15) - (17) are

$$k_o = 0.564 \times 10^{-20} \lambda_o N_L f_{Lu} (\bar{v}_a/c)^{-1}, \text{ cm}^{-1} \qquad (21)$$

$$\Delta\lambda_D = 1.474 \lambda_o (\bar{v}_a/c) \quad , \text{ A}^o \qquad (22)$$

$$\Delta\lambda_C = 2 \times 10^{-16} w N_e \quad , \text{ A}^o \qquad (23)$$

and the absorption coefficient at the line center is

$$k_{\nu_o} = k_o \text{ erfc } \chi \exp \chi^2 \qquad (24)$$

where

$$\chi \approx (\ell n 2)^{1/2} (\Delta\nu_C/\Delta\nu_D)$$

$$= 1.13 \times 10^{-16} N_e (w/\lambda_o) (\bar{v}_a/c)^{-1} \qquad (25)$$

In these results and those which follow, we have used the dimensions

w (Å), λ_o (Å), and N_e (cm^{-3}); all other quantities are either dimensionless or appear only in dimensionless ratios. $\bar{v}_a$ is the mean atom thermal speed $(8kT_a/\pi m_a)^{1/2}$. The natural half-width $\Delta\nu_N$ has been neglected in arriving at Eq. (25), based on the arguments following Eq. (18).

For dominant Stark broadening, i.e. $\chi \gg 1$, the asymptotic form of Eq. (26) is

$$k_{\nu_o} = (\pi^{1/2}\chi)^{-1} k_o \left[1 - \frac{1}{2}\chi^{-2} + ---\right]$$

$$\approx 0.282 \times 10^{-4} \lambda_o f_{Lu} (N_L/N_e)(\lambda_o/w), \text{ cm}^{-1} \quad (28)$$

and the absorption profile near the line center has an approximately Lorentzian form[34]

$$k_\nu(\nu) \approx k_{\nu_o} \left[1 + 4(\Delta\lambda/\Delta\lambda_C)^2\right]^{-1} \quad (29)$$

where $\Delta\lambda$ is the distance from the line center. As described by Wiese[34], the wings of the profile are a great deal more complicated than this simple Lorentzian result.

In selecting a suitable laser for exciting a specific atomic transition subject to Stark broadening, care must be taken to account for the shift of the line center towards longer wavelengths. For any

particular isolated line, the shift is proportional to $\Delta\lambda_C$, and for cesium is of the order of the Stark width. These calculations are described by Griem[33] and Wiese[34]. For a discussion of the overlapping between broadened lines, see Stone and Agnew[37].

Table 2 presents the results of typical calculations corresponding to plasma diode conditions. The suitability of a particular transition for pumping depends upon the width of laser lines available for that specific transition and the calculated absorption. The absorption coefficients for excitations starting from the 5D levels depend sensitively on the electron temperature because it determines the density of the absorbing states. Changes of a few hundred degrees Kelvin in the electron temperature could therefore have a significant effect on the diode output caused by laser pumping of 5D levels.

The total absorption coefficient for any particular incident radiation frequency is the sum of the absorption coefficients from all lines which overlap this frequency. For example, incident radiation at 7280 $\mathring{A}$ would induce both $5D_{5/2} \rightarrow 6F_{7/2}$ and $5D_{5/2} \rightarrow 6F_{5/2}$ transitions because the two lines differ in wavelength by only 0.05 $\mathring{A}$. The oscillator strengths f_{Lu} for these two

transitions are identical[36] and consequently the total absorption coefficients for 7280 Å radiation are twice the values listed in Table 2 for the $5D_{5/2} \rightarrow 6F_{7/2}$ transition alone.

D. Other Optical Pumping Schemes

Several years ago Gibbons[31] performed an experiment to determine the effects of high-intensity broad-band radiation on converter performance. He found that the output current of a diode operating with an electron-rich emitter increased by an order of magnitude when irradiated with the output of a high-intensity xenon flash lamp. No definitive identifications of the excitation mechanisms were made, although he postulated that a major contribution to the enhanced output arose from the absorption of $6S \rightarrow 6P$ resonance radiation. From our previous discussion of recombination and excitation, it is clear that the absorption of an equal amount of energy in transitions satisfying $k' < s$ and $k'' > s$ would lead to much more efficient ionization.

The only other studies reported in the literature involving interaction between the interelectrode plasma and external radiation have been concerned with diagnostics (Refs. 14, 18, 29, 30, 37, 39, 41, and 42). Neither the plasma parameters nor the incident intensity of these investigations were suitable for observing significant enhancement of the plasma density and diode output power.

III. LASER REQUIREMENTS AND CONVERTER EFFICIENCY

In the previous Section the details of photoexcitation and recombination were reviewed from the point of view of selecting transitions favorable to laser pumping. It remains to be demonstrated that suitable laser sources exist and are compatible with the energy requirements of thermionic diodes. At the conclusion of this Section we speculate as to the modifications in diode performance which might be achieved by intense laser excitation.

A. Laser Sources

In discussing laser sources suitable for excitation of diode plasmas, it is important to distinguish between the requirements of laboratory experiments and those of self-contained operational systems. For example, a Raman-shifted ruby laser line might be convenient for the laboratory but far too inefficient

for a practical converter. In contrast, a semi-conductor laser might be desirable for a self-contained system because of its efficient conversion of electrical energy to laser radiation, but extremely awkward to use in the laboratory. A direct analogy exists in present converter technology whereby the nuclear thermal energy of an operational system is simulated by electrical heating.

A closed converter system employing laser pumping would utilize part of the electrical output of the diode to drive the laser. Obviously, one of the most important requirements is efficient conversion of electrical to light energy. Semi-conductor compounds are the only competitive laser sources from this standpoint which are presently available. GaAs is the most efficient of these materials, having a conversion efficiency of up to 80% at $77^{o}K$. Several other compounds have exhibited efficiencies in the neighborhood of 5-20%[43]. Because of the active development presently going on in the semi-conductor laser field (particularly in the investigation of the effects of crystal purity) it is to be expected that subsequent results will outmode the present discussion.

GaAs, a favorable example of semi-conductor lasers suitable for converter excitation, has several interesting properties in addition to a high conversion efficiency. First, the radiation bandwidth is relatively narrow, on the order of $1\,\mathring{A}$ at $77\,^{o}K$ and

5 Å at 300 °K [44]. Second, the output wavelength is tunable by (1) temperature variation, (2) changes in impurity concentration, (3) changes in composition, and (4) the application of pressure or a magnetic field. And third, the diodes are extremely compact, occupying less than 1 cm^3 for an average output power of 10 mW.

Wavelength tuning is particularly important to this application because a precise match must be achieved between the shifted and broadened atomic excitation and the laser pump light. Pure GaAs can be temperature-tuned from about 8450 Å (77 °K) to 9050 Å (300 °K) although the conversion efficiency drops to 2-5% at room temperature. Superimposed on this variation is a shift in output wavelength by ±85 Å with different impurity concentrations. Ternary compounds offer an additional method of wavelength variation; the combination $GaAs_xP_{1-x}$ ($0.5 \lesssim x \leq 1$) at 77 °K would cover the spectral range 6300 Å to 8450 Å. Fine tuning via magnetic fields is possible but has not been extensively investigated.

The wavelength region covered by these tuning mechanisms, approximately 6300 Å to 9100 Å, includes seven of the favorable atomic transitions listed in Table 2. A highly-efficient laser pumping source is therefore realizable within the present state of the art. By utilizing suitable input current waveforms, it should be possible

to minimize the wavelength shift during each output pulse of the laser. For typical commercial GaAs units, this shift is on the order of 25 $\mathring{A}/\mu sec$.

The laboratory investigation of laser pumping exhibits an entirely different set of requirements. The laser source must be sufficiently powerful to assure high power inputs to the diode even for conditions where $k_{\nu_o} \ll 1$ and a single pass of the laser light through the diode is utilized. Several different transitions should be accessible to study without expensive or difficult modifications. And third the laser lines should be broad enough or tunable enough to allow investigation of the excitation line shape under varying plasma conditions.

A brief survey of known discrete laser wavelengths has revealed several near coincidences with atomic cesium transitions. These are listed in the last column of Table 1. The transition $5D_{3/2} \rightarrow 10F_{5/2}$ ($\lambda_o = 6326\ \mathring{A}$) is particularly interesting because the broadened line will overlap the He-Ne wavelength 6328 $\mathring{A}$. There is also a near coincidence between the ruby second harmonic (3471.5 $\mathring{A}$ at 20 ^{o}C) and the $6S_{1/2} \rightarrow 10P_{3/2}$ transition ($\lambda_o = 3477\ \mathring{A}$); a Q-switched ruby passed through ADP or other nonlinear medium would produce upwards of 2 MW of second harmonic radiation for times on the order of 10 ns. Absorption of the 3472 $\mathring{A}$ radiation

would occur in the wings of the absorption line, with an absorption coefficient on the order of 1/10 to 1/100 of the value k_{ν_o} listed in Table 2.

The use of a Q-switched ruby laser with known Raman-active substances[45] will also yield several shifted lines which overlap cesium transitions. Since the half-widths of the shifted lines are on the order of 2 to 40 cm^{-1}, any coincidence within the half-width of the Raman-shifted line will yield acceptable incident power densities for laboratory purposes. Table 3 lists several combinations of interest. Stokes lines are considerably more intense than the anti-Stokes lines, with intensities of up to 30% of the incident beam.

Perhaps the most versatile laboratory system for investigating diode excitation is a parametric oscillator configuration.[46,47] By using advanced nonlinear optical mediums[48,49] such as $Ba_2\ Na\ Nb_5\ O_{15}$, tunable outputs in both CW and pulsed modes can be achieved. The tunable frequency interval is centered about an output wavelength which is twice the input, or "pump", wavelength and covers the approximate range $1.4\ \lambda_{IN} \lesssim \lambda_{OUT} \lesssim 4\ \lambda_{IN}$. Two particularly interesting pumping sources are a pulsed N_2 laser ($3371\ \mathring{A}$)[49,50] and a similar neon laser operating at $5401\ \mathring{A}$[50]. CW outputs in the visible and near infrared should also be possible

using commercially-available ion lasers as pumping sources.

All of the 5D → nF transitions of Table 2 would be amenable to excitation by parametric oscillation outputs from either a pulsed N_2 or a ruby second-harmonic pump source. Although the nonlinear medium KDP is transparent down to 2800 Å (and hence admits the use of both the 3371 Å N_2 line and the 3472 Å ruby second harmonic), some of the more favorable crystals for optical parametric oscillation do not transmit at these low pump wavelengths. $Ba_2NaNb_5O_{15}$, for example, is transparent from 4000 Å to 5 μ[48].

B. Ion Loss Mechanisms and Energy Requirements

There are normally two approaches exhibited in analyses of thermionic converters. The first is a crude order-of-magnitude analysis which assumes spatial independence and appropriate average values of the relevant plasma parameters and makes performance estimates based on these numbers. The second is a detailed calculation which places proper emphasis on the coupling between the sheath conditions and the plasma, transport processes, and (usually) the energy dependence of collision cross sections. We believe that the first (crude) approach is justified in the present exploratory investigation.

For the purposes of a simple illustrative calculation, we assume a diode spacing of 0.03 cm and a diode width of 2 cm. The

undisturbed plasma conditions are taken to be $T_a = 1500\ ^{o}K$, $T_e = 2500\ ^{o}K$, and $N_o = 5 \times 10^{15}\ cm^{-3}$ so that the Saha equilibrium electron density N_e is $1.5 \times 10^{14}\ cm^{-3}$. (The actual electron density would probably be slightly lower than the Saha value, say $N_e = 0.3$ to $1.0 \times 10^{14}\ cm^{-3}$, because of the escape of line radiation from the plasma.) We wish to raise the electron density to $5 \times 10^{14}\ cm^{-3}$ by laser excitation.

Electron-ion loss rates from recombination can be estimated from the experiments of Aleskovskii[40] and others. For high plasma densities the recombination is approximately proportional to N_e^3, and using a two-body recombination coefficient $\alpha = 2 \times 10^{-9}\ cm^3/sec.$ at $N_e = 5 \times 10^{14}\ cm^{-3}$ and $T_e = 0.21$ eV we obtain

$$-\frac{dN_e}{dt} = 5.0 \times 10^{20}\ cm^{-3}\ sec^{-1}$$

The only other ion loss mechanism which is relevant to this crude discussion is diffusion to the electrodes. Spitzer's coulomb self-collision length[52] for these conditions is approximately 6×10^{-4} cm or 1/50 of the electrode spacing. Therefore, both coulomb collisions and ion-neutral charge-exchange collisions will effectively inhibit diffusion and as a first approximation we neglect this loss mechanism.

The rate of laser-produced transitions satisfying $k' < s$ and $k'' > s$ must be nearly equal to the recombination rate. Choosing the wavelength 8081 $\mathring{A}$, both the $5D_{5/2} \rightarrow 5F_{5/2}$ and $5D_{5/2} \rightarrow 5F_{7/2}$ transitions will be excited yielding an effective absorption coefficient $k^*_{\nu_o} = 0.27 \ cm^{-1}$. The attenuation per pass across the 2 cm wide diode is therefore 18%, and by using a reflecting cavity with 3 passes through the diode, we obtain a total absorption of 80%. (In principle it should be possible to position the plasma within the laser cavity and have the absorption represent the full output, or loss, of the cavity. This would be extremely difficult in practice.)

A $GaAs_xP_{1-x}$ laser at 77 ^oK with an efficiency of roughly 60% is a suitable source of this wavelength. The total laser power input required to maintain the plasma density of $5 \times 10^{14} \ cm^{-3}$ would therefore be 7.6 watts per cm^2 of emitter surface area. This is the same order of magnitude as the power one might expect to produce from the diode. The fraction of this power appearing as absorbed laser energy is not "lost" from the plasma. It will appear as excess energy carried away by the free electrons during three-body recombination and therefore increase the electron temperature. The higher electron temperature, in turn, will increase the electron density and hence the preceding power estimate may be higher than

is actually required to sustain the desired electron density.

C. Modifications of Diode Performance with Laser Pumping

It is extremely difficult to construct an accurate picture of diode performance under the action of strong laser pumping without detailed plasmadynamic calculations, experiments, or both. One difficulty (which is often overlooked in converter theory) is that the neutral number density varies significantly across the interelectrode gap. For a constant cesium pressure, $N_o \propto T_a^{-1}$ and T_a decreases from the hot emitter side of the diode to the cold collector. As a first estimate, therefore, one would expect significantly more laser radiation absorption near the collector.

The effects of differential absorption rates across the diode are difficult to decipher. They will obviously depend upon the particular "mode" of operation[1], i.e. on the "undisturbed" interelectrode potential distribution prior to laser excitation. A preliminary estimate, based on a consideration of particle flux balances across the emitter and collector sheaths, suggests that both the output voltage and output current will increase with laser excitation. The increased current comes primarily from an increase in the plasma density near the collector and hence the random electron particle flux $j_r = N_e \bar{v}_e/4$. In the case of an "obstructed

mode" with a double sheath at the emitter[1], increasing the plasma density near the emitter will lower the initial potential barrier to electron flow and a larger fraction of the emitter saturation current will flow into the plasma.

The output voltage of the device should increase on two counts. First, the neutral density necessary to sustain a given current will be reduced, thereby decreasing the electron-neutral contribution to plasma resistivity. The total plasma resistivity drop in conventional diodes is on the order of 1 to 3 kT_e, i.e. about equal to the converter output voltage. In addition, the magnitude of the potential accelerating emitter electrons into the plasma will be decreased. As mentioned in the Introduction, these accelerated electrons are primarily responsible for the collisional ionization which sustains the conventional ignited-mode plasma density. The laser-pumped diode relies primarily on photo-excitation of states $k' < s$ to $k'' > s$, and the role of the electron temperature (aside from its influence on $\bar{v}_e$) is to supply a sufficient number density $N_{k'}$ of absorbing states. It should be emphasized that most of the laser power pumped into the plasma is not "lost" but converted into random thermal energy of the electrons during the recombination process.

IV. CONCLUSIONS

The preceding analysis has indicated that laser excitation of cesium-filled thermionic converters may lead to substantial increases in output power density and efficiency when compared to conventional devices operating in the ignited mode. Furthermore, the most efficient laser excitation wavelengths for producing ionization have been identified, and a semi-quantitative estimate has been made of the power input required to sustain a given plasma density.

However, it has not been possible to make a detailed analysis of the coupling between the enhanced plasma density and the diode output. This coupling depends on the detailed absorption distribution of the incoming radiation, the effect of enhanced recombination rates on the electron temperature, and on the effects of the altered plasma properties on the emitter and collector sheaths. Consequently, careful laboratory measurements will have to be conducted to experimentally ascertain the feasibility of this technique.

ACKNOWLEDGEMENTS

This investigation was sponsored jointly by the U. S. Atomic Energy Commission (Contract AT(11-1)-1776) and the Air Force Flight Dynamics Laboratory (Contract F 33615-67-C-1850). We wish to express our appreciation to Dr. George Miley of the University of Illinois for bringing References 31 and 42 to our attention and enlightening subsequent discussion; and also to the BUILD Cooperative Program between the University of Illinois and the University of Colorado which made these discussions possible.

REFERENCES

1. R. H. Bullis et al, J. Appl. Phys., 38, 3245 (1967).

2. H. L. Witting and E. P. Gyftopoulos, J. Appl. Phys., 36, 1328 (1965).

3. L. P. Harris, J. Appl. Phys., 36, 1543 (1965).

4. K. G. Hernqvist, Proc. IEEE, 51, 748 (1963).

5. It is important to include ion currents returning to the emitter and Schottky effects in interpreting the diode characteristics; see L. K. Hansen, J. Appl. Phys., 38, 4345 (1967) and D. R. Wilkins, J. Appl. Phys. (to be published).

6. The absorption of other gases such as Barium can also significantly lower the work function; see e.g. J. Psarouthakis, AIAAJ. 4, 1201 (1966).

7. P. L. Auer, J. Appl. Phys., 31, 2096 (1960).

8. R. G. McIntyre, J. Appl. Phys., 33, 2485 (1962); R. G. McIntyre, Proc. IEEE, 51, 760 (1963).

9. P. Burger, J. Appl. Physics, 36, 1938 (1965).

10. S. A. Self, J. Appl. Phys., 36, 456 (1965).

11. H. Heil and B. Scott, Phys. Rev., 145, 279 (1966).

12. K. J. Nygaard, Sperry Rand Research Center, unpublished.

13. L. P. Harris, J. Appl. Phys., 36, 1543 (1965).

14. A recent experiment by Kniazzeda and Carabeteas (Proc. IEEE Thermionic Conversion Specialists Conf., San Diego, 1965, p. 109) has established an upper limit of 0.2×10^{-16} cm^2 for the cross section associated with cesium molecular ion formation, a value four orders of magnitude smaller than the one used by Witting and Gyftopoulos.[2]

15. D. R. Bates, Phys. Rev., 78, 492, (1950).

16. D. R. Wilkins, Report LA-3143-MS (1964), Los Alamos Sci. Lab., Los Alamos, N. M.

REFERENCES (CONTD.)

17. K. E. Harwell and R. G. Jahn, Phys. Fluids, 7, 214 (1964).

18. L. Agnew, Proc. Thermionic Conversion Specialists Conf., San Diego, 25-27 Oct., 1965, pp. 119-125.

19. D. R. Wilkins and E. P. Gyftopoulos, J. Appl. Phys., 37, 2888, (1966).

20. L. K. Hansen and C. Warner, Bull. APS., 12, 986, (1967).

21. D. W. Norcross, Bull. APS., 12, 986, (1967).

22. E. W. McDaniel, Collision Phenomena in Ionized Gases, Wiley, N. Y. (1964), pp. 594 et seq.

23. B. Va. Moizhes, F. G. Basht, and M. G. Melikiya, Sov. Phys. Tech. Phys., 10, 1252, (1966).

24. S. Byron, R. C. Stabler, and P. I. Bortz, Phys. Rev. Lett., 8, 376 (1962).

25. J. V. Dugan, Jr., F. A. Lyman, and I. V. Albers, Electricity from MHD, Vol. II, International Atomic Energy Agency, Vienna, 1966, p. 85. See also J. V. Dugan, Jr., J. Appl. Phys., 37, 5011 (1966).

26. M. J. Zgorzelski, Fluid Mechanics Laboratory Publication, No. 68-1, Mass. Inst. Tech., Cambridge, February, 1968.

27. D. R. Bates, A E. Kingston, and R. P. McWhirter, Proc. Royal Soc. (London), A267, 297 (1962).

28. C. Warner and L. K. Hansen, J. Appl. Phys., 38, 491 (1967).

29. P. D. Foote and F. L. Mohler, Phys. Rev., 26, 195 (1925).

30. F. L. Mohler P. D. Foote, and R. L Chenault, Phys. Rev., 27, 37 (1926).

31. M. D. Gibbons, Proc. IEEE Thermionics Specialists Conf., Gatlinburg, Tenn., 1963, p. 103.

32. The half-width is defined as the full width between half-maximum points of the absorption profile.

33. H. R. Griem, Plasma Spectroscopy, McGraw-Hill, New York, 1964.

34. W. L. Wiese, in Plasma Diagnostic Techniques, R. H. Huddlestone and S. L. Leonard (Eds.), Academic Press, N. Y., 1965, p. 277.

35. R. M. Goody, Atmospheric Radiation I. Theoretical Basis, Oxford University Press, Oxford, 1964, p. 126.

36. P. M. Stone, Phys. Rev., 127, 1151 (1962).

37. P. M. Stone, and L. Agnew, Phys. Rev., 127, 1157 (1962).

38. D. R. Wilkins and E. P. Gyftopoulos, J. Appl. Phys., 37, 2892 (1966).

39. W. H. Reichelt, "Spectroscopic Investigation of the Ignited Mode of Thermionic Converter Operation", International Conference on Thermionic Electric Power Generation, London, England, September, 1965, as requoted in Ref. 38.

40. Yu M. Aleskovskii, Soviet Physics - JETP, 17, 570 (1963).

41. F. L. Mohler and C. Boeckner, Bur. Stds. J. Res., 5, pps. 51, 399, (1930).

42. N. D. Morgulis, Yu P. Korchevoi, and A. M. Przhonsky, Sov. J. Tech. Phys., 53, 417 (1967). (In Russian).

43. F. F. Morehead, Jr., Scientific American, Vol. 216, pp. 109-122, May, 1967. The efficiencies quoted in this article may be somewhat optimistic but are indicative of what may be practical in the near future.

44. These data are taken from specifications for RCA Developmental Type TA 2628 (Dec., 1966) for a single emitting element plus corroborating information from the same laboratory appearing in the literature (see M. F. Lamorte et al., IEEE J. Quant. Elect., QE-2, 9 (1966)). These half-widths are considerably less than those reported by other investigators at equivalent temperatures (B. A. Lengyel, Introduction to Laser Physics, Wiley, N. Y.,

1966, p. 145 . Diode arrays consisting of a number of independent lasing elements in series have considerably larger half-widths, on the order of 40-50 Å. Presumably proper quality control can reduce the array bandwidth to that of a single element.

45. G. Eckhardt, IEEE J. Quant. Elect., QE-2, 1 (1966).

46. J. A. Giordmaine and R. C. Miller, Appl. Phys. Lett., 9, 298 (1966).

47. R. C. Miller and W. A. Nordland, Appl. Phys. Lett., 10, 53 (1967).

48. J. E. Geusic et. al., Appl. Phys. Lett., 11, 269 (1967).

49. K. F. Hulme et. al., Appl. Phys. Lett., 10, 133 (1967).

50. D. A. Leonard, R. A. Neal, and E. T. Gerry, Appl. Phys. Lett., 7, 175 (1965).

51. J. D. Shipman, Jr., Appl. Phys. Lett., 10, 3 (1967).

52. L. Spitzer, Physics of Fully-Ionized Gases, 2nd Ed., Interscience Publ., N. Y., 1962, p. 126.

Table 1. Data on Selected Cesium Transitions

STATES k'	STATES k''	$f(k' \rightarrow k'')^a \equiv f_{Lu}$	w^b (Å)	λ^c (Å)	$E_I - E_{k''}{}^c$ (eV)	Measured Laser Lines[d]
$6S_{1/2}$	$6P_{1/2}$	.394	.0686	8944	2.507	
	$6P_{3/2}$	.894	---	8921	2.438	
	$7P_{1/2}$	.00284	.0161	4593	1.194	
	$7P_{3/2}$	.0174	.0189	4555	1.172	
	$8P_{1/2}$	.000317	.480	3889	.705	
	$8P_{3/2}$	.00349	.574	3876	.695	
$6P_{1/2}$	$7S_{1/2}$	.171	.392	13589	1.594	
	$6D_{3/2}$	.298	.393	8761	1.092	
	$8S_{1/2}$	.0202	.437	7609	.877	
	$7D_{3/2}$	.0927	.988	6723	.663	Oxygen II (6721.4Å)
$6P_{3/2}$	$7S_{1/2}$	.208	.458	14695	1.594	
	$6D_{3/2}$	.0397	---	9208	1.092	
	$6D_{5/2}$	.332	.514	9172	1.086	
	$8S_{1/2}$	.0204	.476	7944	.877	
	$7D_{3/2}$	.0110	---	6984	.663	
	$7D_{5/2}$	.0951	1.28	6973	.660	
$5D_{3/2}$	$7P_{1/2}$	.652	---	13763	1.194	
	$7P_{3/2}$	.208	---	13428	1.172	
	$4F_{5/2}$	.302	(1.8)	10027	.859	
	$5F_{5/2}$	.122	5.67	8018	.548	
	$6F_{5/2}$	.0627	15.7	7229	.380	
	$7F_{5/2}$	.0373	29.4	6825	.280	
	$8F_{5/2}$	.0235	52.0	6586	.214	Iodine II (6585.0Å)
	$10F_{5/2}$	.0114	138.0	6326	.137	He - Ne (6328Å)

Table 1. (con't)

STATES k'	STATES k''	$f(k' \rightarrow k'') \equiv f_{Lu}$ [a]	w [b] (Å)	λ [c] (Å)	$E_I - E_{k''}$ [c] (eV)	Measured Laser Lines [d]
$5D_{5/2}$	$7P_{3/2}$	1.533	---	13606	1.172	
	$4F_{5/2}$	.324	(1.8)	10126	.859	
	$4F_{7/2}$	"	"	"	"	
	$5F_{5/2}$	.127	5.74	8081	.548	
	$5F_{7/2}$	"	"	"	"	
	$6F_{5/2}$	.0650	15.9	7280	.380	
	$6F_{7/2}$	"	"	"	"	
	$7F_{5/2}$	.0383	29.8	6870	.280	
	$7F_{7/2}$	"	"	"	"	
	$8F_{5/2}$	.0241	52.6	6629	.214	
	$8F_{7/2}$	"	"	"	"	

a. From P. M. Stone, Phys. Rev., 127, 1151 (1962).

b. From H. R. Griem, Plasma Spectroscopy, McGraw-Hill, N.Y., 1964. Values in parentheses are estimated by extrapolation. Values are for $T_e = 2500\ ^{o}K$.

c. Computed from C. E. Moore, Atomic Energy Levels, N.B.S. Circular no. 467, Vol. III, pp. 124-130, 1958. λ_o is the vacuum wavelength of the unshifted atomic line.

d. The laser wavelengths have been reported in the current literature [see e.g. W. B. Bridges and A. N. Chester, J. Quant. Elec., I, 66, (1965)]. A summary of laser uses in spectroscopy will be published shortly by the senior author.

Table E. Stark Widths and Absorption Coefficients for Selected Cs Transitions.[a]

k' → k''	λ_o (Å)[b]	T_e = 3000 °K, $N_e = 10^{14}$ cm^{-3}, $N_o = 2 \times 10^{16}$ cm^{-3}		T_e = 3000 °K, $N_e = 10^{15}$ cm^{-3}, $N_o = 2 \times 10^{16}$ cm^{-3}		T_e = 3000 °K, $N_e = 10^{15}$ cm^{-3}, $N_o = 5 \times 10^{15}$ cm^{-3}		T_e = 2500 °K, $N_e = 10^{15}$ cm^{-3}, $N_o = 5 \times 10^{15}$ cm^{-3}	
		$\Delta\lambda_C$ (Å)	k_{ν_o} (cm^{-1})	$\Delta\lambda_C$ (Å)	k_{ν_o} (cm^{-1})	$\Delta\lambda_C$ (Å)	k_{ν_o} (cm^{-1})	$\Delta\lambda_C$ (Å)	k_{ν_o} (cm^{-1})
$6S_{1/2} \rightarrow 8P_{3/2}$	3876	.012	393.5	.115	51.4	.115	12.8	.115	12.8
$\rightarrow 9P_{3/2}$	3612	.029	61.8	.290	6.33	.290	1.58	.290	1.58
$\rightarrow 10P_{3/2}$	3477	.063	13.4	.634	1.34	.634	.334	.634	.334
$\rightarrow 11P_{3/2}$	3398	.122	3.81	1.22	.381	1.22	.095	1.22	.095
$\rightarrow 12P_{3/2}$	3347	.218	1.21	2.18	.121	2.18	.030	2.18	.030
$5D_{3/2} \rightarrow 6F_{5/2}$	7229	.314	2.26	3.14	.226	3.14	.056	3.14	.014
$\rightarrow 8F_{5/2}$	6596	1.04	.213	10.4	.021	10.4	.0053	10.4	.0013
$\rightarrow 10F_{5/2}$	6326	2.76	.036	27.6	.0036	27.6	.00089	27.6	.00022
$5D_{5/2} \rightarrow 5F_{7/2}$	8081	.115	22.0	1.15	2.20	1.15	.550	1.15	.135
$\rightarrow 6F_{7/2}$	7280	.318	3.29	3.18	.329	3.18	.082	3.18	.021
$\rightarrow 7F_{7/2}$	6870	.596	.925	5.96	.093	5.96	.023	5.96	.0057
$\rightarrow 8F_{7/2}$	6621	1.05	.306	10.5	.031	10.5	.0076	10.5	.0019
		$(N_e)_{SAHA} = 1.53 \times 10^{15}$ cm^{-3}		$(N_e)_{SAHA} = 1.53 \times 10^{15}$ cm^{-3}		$(N_e)_{SAHA} = 7.65 \times 10^{14}$ cm^{-3}		$(N_e)_{SAHA} = 1.50 \times 10^{14}$ cm^{-3}	

a. For conditions where $\Delta\lambda_C$ and $\Delta\lambda_D$ are of the same order, an atom temperature of 1500 °K was assumed to calculate $\bar{v}_a$ appearing in Eq. (26).

b. Vacuum wavelength of the unshifted line.

Table 3. Overlaps between Raman-Shifted Ruby Laser Lines and Cesium Atomic Transitions

Cesium Transition		Ruby Source[a]			Raman Substance[b]		
$k' \rightarrow k''$		λ_o (Å)	T (°K)	λ_L (Å)	Material	$\Delta\nu$ (cm^{-1})	Shift
$6S_{1/2} \rightarrow$	$8P_{3/2}$	3876	293	3472	paraxylene	2998	S_1
	$9P_{3/2}$	3612	293	3472	calcite	1086	S_1
	$10P_{3/2}$	3477	293	3472	none	0	-
	$11P_{3/2}$	3398	293	3472	carbon disulfide	655	AS_1
	$12P_{3/2}$	3347	293	3472	calcite	1086	AS_1
$5D_{3/2} \rightarrow$	$6F_{5/2}$[c]	7229	77	6934	carbon disulfide	655	S_1
	$8F_{5/2}$	6586	77	6934	orthoxylene	730	AS_1
	$10F_{5/2}$	6326	77	6934	napthalene	1380	AS_1
$5D_{5/2} \rightarrow$	6F	7280	293	6943	chloroform	663	S_1
	8F	6629	77	6934	chloroform	663	AS_1
$6P_{1/2} \rightarrow$	$6D_{3/2}$	8761	293	6943	1,1,2,2, tetrachloroethane	2984	S_1
					deuterium	2991	S_1
$\rightarrow$	$7D_{3/2}$	6723	293	6943	α - sulfur	470	AS_1

(a) The lines λ_L = 3467 Å and 3472 Å are ruby second harmonics at 77 °K and 293 °K respectively.

b) From G. Eckhardt, IEEE J. Quant. Elect., QE-2, 1 (1966). S_1 designates the first Stokes shift and AS_1 designates the first anti-Stokes shift.

(c) The indicated shifted laser line exceeds λ_o by 34 Å.

FIGURE CAPTIONS

Fig. 1. Energy Level Diagram for Cesium

Fig. 2. Schematic Illustration of the Effect of Laser Excitation on Excited State Populations

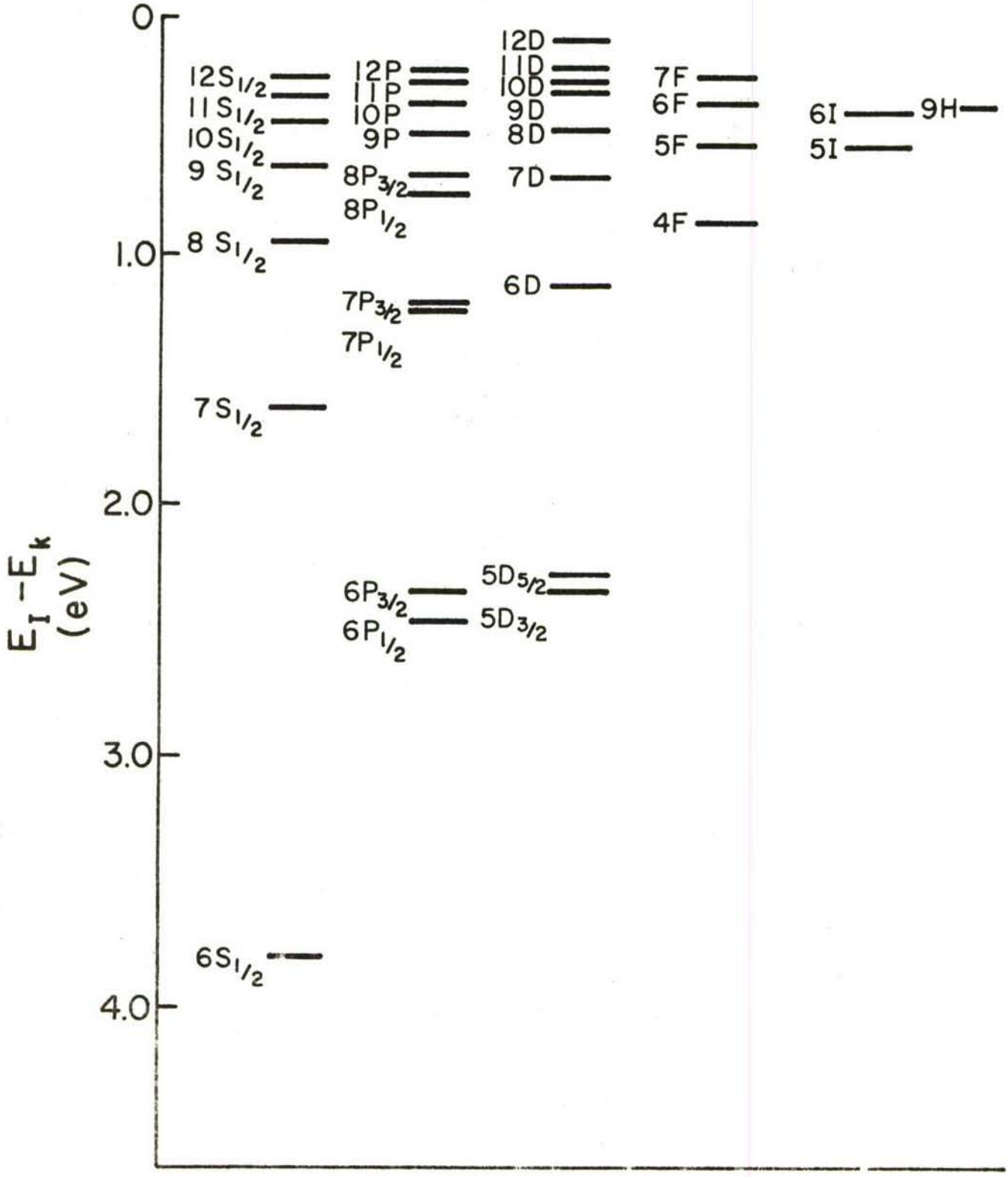

Fig. 1. Energy Level Diagram for Cesium

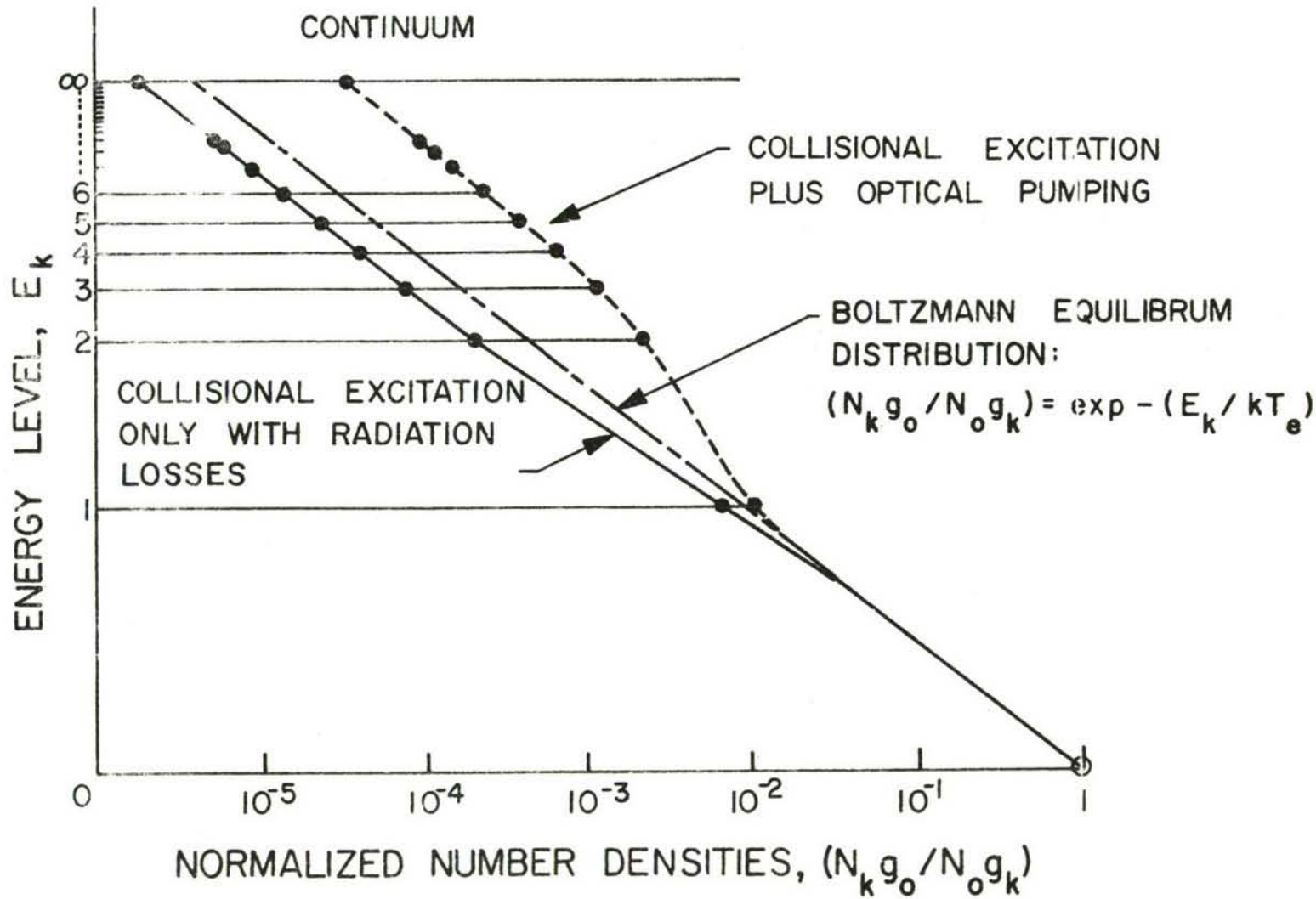

Fig. 2. Schematic Illustration of the Effect of Laser Excitation on Excited State Populations

ATTACHMENT C

A NEW TECHNIQUE FOR JOINING POROUS REFRACTORY METALS

by

C. Forbes Dewey, Jr.*
University of Colorado, Boulder, Colorado

There are two important aerospace applications of porous refractory metals and their alloys: as ionizers in electrostatic thrustors and as rocket nozzle liners in sacrificial cooling systems. It is useful in both of these applications to be able to employ matricies having a wide spectrum of permeabilities.

The three previous methods of joining porous refractory materials to supporting metal structures have been direct electron-beam welding in a vacuum[1], arc welding in a high-purity inert atmosphere, and brazing. Achieving success with the first two of these methods is an art as best, and to the writer's knowledge no satisfactory results have been obtained

---

*Present Address: Department of Mechanical Engineering, Massachusetts Institute of Technology, Cambridge, Massachusetts.

when the void fraction of the porous material excees 28%. Brazing techniques often exhibit disadvantages in these applications; for example, high-temperature diffusion of braze material into an ionizer may lead to undesirable surface ionization properties.[2]

Fig. 1 illustrates the technique which was developed for joining a high-porosity tungsten-tantalum matrix to a thin solid tantalum support structure. The porous material was first machined to size using conventional techniques, being sure that the exposed surface was free of fractured material. A thin coating of tantalum was then applied using a vapor-deposition process. A final weld was then consummated between the coating material and the support structure.

The vapor-deposited coating exhibits a semi-matallurgical, semi-mechanical bond with the porous material. Shear strength parallel to the coating-porous matrix interface should equal that of the matrix itself, while the joint tensile strength is of the same order as the matrix. We have operated the assembly shown in Fig. 1 at 2100 ^{o}K and above for extended periods of time without any indication of mechanical failure. During this operation, the joint was subject to shear forces of 35 psi and thermally-induced tensile forces of about three times this value. (One unit was subject to severe thermal shock because of a power failure to the heating system. The porous button cooled rapidly because of its high emissivity and cracking of the porous matrix occurred. The vapor deposition area, however, remained in sound condition with no evidence of mechanical failure of the vapor deposit-porous matrix interface.)

Both laser welding and arc welding in an inert atmosphere have been successfully used to join the tantalum support to the vapor-deposited coating. Electron-beam welding should also be possible. Laser welding offers a distinct advantage in this application because no significant heating of the parts is encountered. Thin materials can be joined to massive sections without distortion or elaborate fixturing. We have produced continuous Ta-Ta seam welds by overlapping spots from a pulsed ruby laser in an inert atmosphere, and the resulting joints have shown no porosity when tested on a sensitive leak detector. Our experience with tungsten-tantalum welds has been very discouraging. The weld material exhibits microscopic brittle fracture under conditions which have produced sound tungsten-tungsten and tantalum-tantalum welds.

The stability of the joint between the vapor-deposited coating and the porous material suggests that large-scale composite structures can be manufactured by vapor deposition. A wide variety of combinations of vapor-deposited coatings and porous materials should prove feasible. Tungsten vapor deposition is a well-developed technique, and would be suitable for pure tungsten matricies. It should be possible, for example, to fabricate a rocket nozzle liner having porous tungsten inserts with the same vapor deposition techniques currently used to produce impervious tungsten liners.

ACKNOWLEDGEMENTS

This work was supported in part by the Atomic Energy Commission Contract AT(11-1) - 1776, and in part by the U. S. Air Force (AFSC),

ACKNOWLEDGEMENTS

Contract F 33615-67-C-1850. The assistance of the following individuals during the fabrication of the unit depicted in Fig. 1 is gratefully acknowledged: Roger Turk of the Hughes Research Laboratory, Malibu, California; Philip Bruno of the Norton Metals Divison, Newton, Massachusetts; and Dale Hansen of the University of Colorado.

REFERENCES

1. S. Robelotto, "Electron-Beam Welding of Refractory Materials for Ion Propulsion System," Proc. 5th Electron Beam Symposium, J. R. Morey (Ed.), Alloyed Electronics Corp., Cambridge, Mass., 1963, pp. 219-229.

2. D. F. Hall, A. Y. Cho, and H. Shelton, "An Experimental Study of Porous Metal Ionizers," AIAA Paper No. 66-218, March, 1966.

FIGURE CAPTION

Fig. 1. Fabrication Procedure for Porous Ionizers.

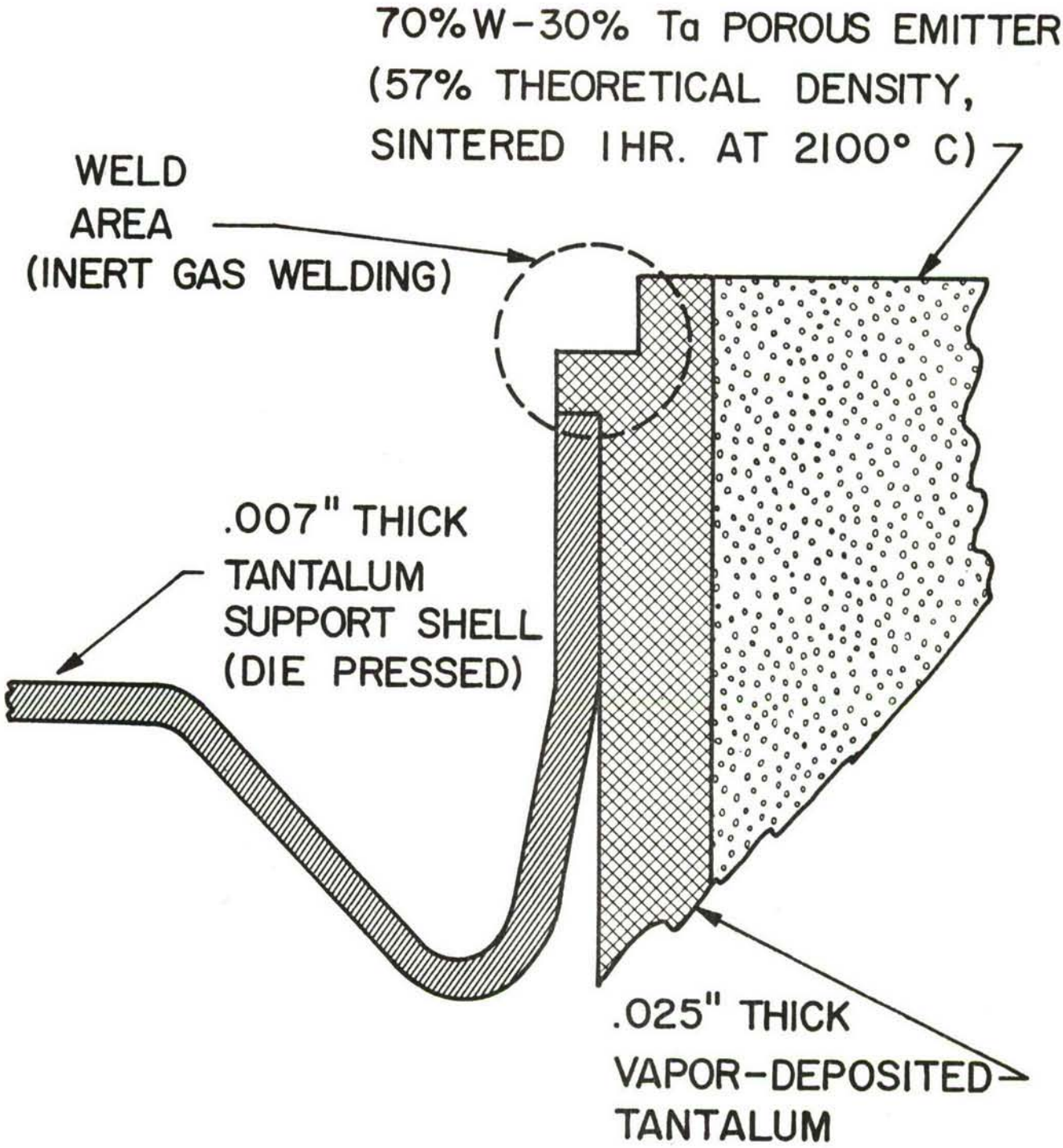

Fig. 1. Schematic Illustration of Fabrication Procedure for Porous Ionizer.

Unclassified

Security Classification

DOCUMENT CONTROL DATA - R & D

(Security classification of title, body of abstract and indexing annotation must be entered when the overall report is classified)

1. ORIGINATING ACTIVITY *(Corporate author)*
University of Colorado
Boulder, Colorado 80302

2a. REPORT SECURITY CLASSIFICATION
Unclassified

2b. GROUP

3. REPORT TITLE

Plasma Diagnostic Methods for Ionized Gas Flows

4. DESCRIPTIVE NOTES *(Type of report and inclusive dates)*
Final Technical Report

5. AUTHOR(S) *(First name, middle initial, last name)*

C. Forbes Dewey

6. REPORT DATE	7a. TOTAL NO. OF PAGES	7b. NO. OF REFS
March, 1969	118	Attach A - 67, Att. B-52, Att. C - 2

8a. CONTRACT OR GRANT NO.	9a. ORIGINATOR'S REPORT NUMBER(S)
F33 615-67-C-1850	Final Technical Report
b. PROJECT NO. 26692	
c.	9b. OTHER REPORT NO(S) *(Any other numbers that may be assigned this report)*
d.	

10. DISTRIBUTION STATEMENT
This document has been approved for public release and sale; its distribution is unlimited.

11. SUPPLEMENTARY NOTES	12. SPONSORING MILITARY ACTIVITY
	Air Force Flight Dynamics Laboratory Air Force Systems Command Wright-Patterson AFB, Ohio

13. ABSTRACT An investigation has been conducted to elucidate several different methods of diagnostics for ionized gas flows. Particular emphasis was placed on techniques of possible interest to the 50 Megawatt Facility at Wright Field. An analysis was completed which describes the behavior of Langmuir probes in strong magnetic fields. The detailed behavior of the results indicates that the theory is capable of describing, with reasonable quantitative accuracy, the collection properties of Langmuir probes as a function of applied potential and magnetic field strength for all magnetic fields $B > 0$. Thomson scattering measurements of electron density do not appear feasible for the 50 Megawatt Facility for two reasons. First, the large fluctuations in plasma density (from less than 10^5 to approximately 10^{12} cm^{-3}) measured in the facility during the time period of this contract makes Thomson scattering an extremely difficult measurement to perform (the lower limit of electron density for Thomson scattering is roughly 10^{12} cm^{-3}). And second, the estimated contamination levels (on the order of 10^{-2} to 10^{-1} wt. percent of contaminants) would introduce spurious signals which will be of the same order as the electron scattering. An analysis was made of several types of atomic and molecular flourescence radiation experiments of potential diagnostics use in the 50 Megawatt Facility. It is concluded that local specie concentration measurements of NO and O_2 can be accomplished using laser flourescence excitation, and that gas velocity measurements can be made using laser excitation of the N_2 Lyman-Birge-Hopfield system or the NO (β) system and monitoring the trajectory of the excited volume of gas. Additional work completed during contract and described herein is as follows: 1) A novel method of "pumping" energy conversion devices with lasers to achieve enhanced electrical output. 2) A general survey of laser sources for line spectroscopy. 3) A new method of joining porous refractory metals. 4) Laser welding.
This abstract may be further distributed by any holder without specific prior approval.

DD FORM 1 NOV 65 1473

Unclassified

Security Classification

14 KEY WORDS	LINK A		LINK B		LINK C	
	ROLE	WT	ROLE	WT	ROLE	WT
Plasma Diagnostics						
Velocity Measurements						
Density Measurements						
Laser Spectroscopy						
Laser Welding						
Thermionic Energy Converter						